PB 181505
Price $2.25

9

LOW-CYCLE FATIGUE BEHAVIOR OF AXIALLY LOADED SPECIMENS OF MILD STEEL

SSC-151

BY

J. T. P. YAO AND W. H. MUNSE

SHIP STRUCTURE COMMITTEE

Distributed by

U.S. DEPARTMENT OF COMMERCE
OFFICE OF TECHNICAL SERVICES
WASHINGTON 25, D. C.

SHIP STRUCTURE COMMITTEE

MEMBER AGENCIES:

BUREAU OF SHIPS, DEPT. OF NAVY
MILITARY SEA TRANSPORTATION SERVICE, DEPT. OF NAVY
UNITED STATES COAST GUARD, TREASURY DEPT.
MARITIME ADMINISTRATION, DEPT. OF COMMERCE
AMERICAN BUREAU OF SHIPPING

ADDRESS CORRESPONDENCE TO:

SECRETARY
SHIP STRUCTURE COMMITTEE
U. S. COAST GUARD HEADQUARTERS
WASHINGTON 25, D. C.

24 June 1963

Dear Sir:

The Ship Structure Committee is sponsoring a project at the University of Illinois to evaluate the influence of a few load cycles at high-stress levels upon the mechanical properties of ship steels. Herewith is a copy of the Third Progress Report, SSC-151, Low-Cycle Fatigue Behavior of Axially Loaded Specimens of Mild Steel by J. T. P. Yao and W. H. Munse.

This project is being conducted under the advisory guidance of the Committee on Ship Structural Design of the National Academy of Sciences-National Research Council.

This report is being distributed to the individuals and agencies associated with the project, and to those interested in the Ship Structure Committee program. Questions or comments regarding this report would be appreciated and should be sent to the Secretary, Ship Structure Committee.

Sincerely yours,

T. J. FABIK
Rear Admiral, U. S. Coast Guard
Chairman, Ship Structure Committee

Serial No. SSC-151

Third Progress Report
on
Project SR-149

to the

SHIP STRUCTURE COMMITTEE

on

LOW-CYCLE FATIGUE BEHAVIOR OF AXIALLY LOADED SPECIMENS OF MILD STEEL

by

J. T. P. Yao and W. H. Munse
University of Illinois

under

Bureau of Ships
Department of the Navy
Contract NObs-77139

transmitted through

Committee on Ship Structural Design
Division of Engineering and Industrial Research
National Academy of Sciences-National Research Council

under

Department of the Navy
Bureau of Ships Contract NObs-84321

Washington, D. C.
U. S. Department of Commerce, Office of Technical Services

24 June 1963

ABSTRACT

Studies have been conducted to evaluate the low-cycle high-stress fatigue behavior of several ship steels under a variety of loading conditions. On the basis of these tests and related studies reported in the literature a general hypothesis describing the cumulative effect of plastic deformations has been developed. With this hypothesis the deformation obtained in a single loading may be used to describe or predict the basic low-cycle fatigue behavior of mild steels for lives up to approximately 1,000 cycles. Furthermore, limited correlations with existing data from other investigations suggest that it may also be possible to extend the hypothesis to metals other than steel.

CONTENTS

SR-149 PROJECT ADVISORY COMMITTEE

"Low-Cycle Fatigue"

for the

COMMITTEE ON SHIP STRUCTURAL DESIGN

Chairman:

J. M. Frankland
National Bureau of Standards

Members:

J. A. Bennett
National Bureau of Standards

B. J. Lazan
University of Minnesota

J. D. Lubahn
Colorado School of Mines

Dana Young
Southwest Research Institute

I. INTRODUCTION

1. General Problem

For over one hundred years investigators have been obtaining fatigue data from specimens of various configurations, made of numerous types of materials, and under many different test conditions. As a result, a vast amount of data are available. However, most of these data are for specimens that failed only after a great many applications of load.

Although fatigue failures generally occur in members that are subjected to many applications of relatively low nominal stresses, unusually high stresses may occasionally be encountered in some structures and result in failure at a relatively small number of cycles. In such cases the stresses or strains will no doubt be large, generally sufficient to cause yielding. As a result, the question of high-stress low-cycle fatigue has become important in many fields.

During the last two decades a large amount of information on the low-cycle fatigue behavior of metals has been published[1], the distinction between low-cycle and long-life fatigue being made arbitrarily on the basis of the number of load applications to failure. The upper limit of life in low cycle fatigue has generally been selected by various investigators to lie in the range of 10^4 to 10^5 cycles. On the other hand, the lower limit of life in a low-cycle fatigue test is the static tensile test which is found to be represented as 1/4, 1/2, 3/4 or one-cycle depending upon the stress-cycle (or strain-cycle) studied or the individual investigator's interpretation or preference.

Since the boundary between low-cycle and long-life fatigue is arbitrarily defined, no precise distinction can be made between these two designations. Furthermore, in low-cycle fatigue tests the loads are generally controlled in terms of either load, stress or deformation. For this reason, all low-cycle fatigue tests need to be further identified as constant-load, constant-stress or constant-deformation tests. Although most studies have been conducted with either constant-load or constant strain tests, a limited number of exploratory tests have been conducted[2] by controlling limits of "true stress." In spite of the fact that extreme care was exercised in monitoring these "true stress" limits, a relatively large scatter was obtained in the test results due to the difficulty of controlling the "true stress."

In general the results of constant-load low-cycle fatigue tests are presented in the form of conventional s-n curves where s and n are respectively the maximum engineering stress or stress range and the corresponding life of the specimens. Although the shape of a typical s-n curve for low-cycle tests can be qualitatively described, it is difficult to make any precise analysis of the test results at the lower numbers of cycles. On the other hand, the results of constant-deformation low-cycle fatigue tests have shown consistently that a linear log-log relationship exists between the change in deformation and the number of cycles to failure.

Empirical relationships have been developed to describe the effect of fully-reversed cyclic strain on the low-cycle fatigue life of metals. These relationships, however, are not suitable to analyze the data of low-cycle fatigue tests in which the cyclic changes in plastic strain are not fully-reversal. In the latter type of test the total plastic strain at failure is found to increase with the number of cycles.

2. Object and Scope

The current research program was initiated to investigate the behavior

of ship steels under low-cycle fatigue conditions. To achieve this objective, the program has been divided into the following four phases: (a) a review of available information in this field, (b) studies of small coupon-type specimens, (c) studies of notched plate specimens, and (d) studies of welded specimens.

This report summarizes the work done on the second phase of this project, namely the studies of the low-cycle fatigue behavior of small coupon-type specimens. The primary purpose of this phase of the program is to develop a general low-cycle fatigue hypothesis and, in the process, to conduct limited studies on a number of the factors which may affect this hypothesis, such as type of test, mode of failure, material, specimen geometry and load cycle. Consequently, many of the parameters discussed in this report will not or cannot be evaluated fully. Nevertheless, they have been evaluated insofar as possible and often related to other similar information in the literature.

In the program three types of tests, namely one-cycle, cyclic load, and cyclic deformation tests, were carried out on eleven types of specimens made of ABS-C normalized, ABS-C as-rolled, and a rimmed steel. Approximately 240 specimens were tested under a variety of loading conditions.

On the basis of a study of published work on low-cycle fatigue, a general hypothesis was developed to describe the cumulative effect of plastic strains on the low-cycle fatigue behavior of metals. This hypothesis takes into account such factors as the compressive plastic deformation, the tensile plastic deformation, and the number of cycles to failure, and has been verified by test data of the present investigation. In addition, limited correlations with published test data from other types of low-cycle fatigue tests on aluminum alloy 2024 were made and indicate that it may well be possible to extend the hypothesis to metals other than mild steel.

3. Acknowledgement

The tests and analysis reported herein were conducted in the Structural Research Laboratory of the Department of Civil Engineering, University of

Illinois, as a part of the Low-Cycle Fatigue program sponsored by the Ship Structure Committee under the Department of the Navy, Bureau of Ships, Contract NObs 77008, Index No. NS-731-034. A committee consisting of Dr. J. M. Frankland, Chairman, Mr. John Bennett, Professor B. J. Lazan, Dr. J. D. Lubahn and Dr. Dana Young has served in an advisory capacity for this program.

The authors wish to express their appreciation to Professor R. J. Mosborg, Professor V. J. McDonald, and Dr. S. T. Rolfe, formerly Research Associate in Civil Engineering, for their helpful suggestions in many phases of this research. Special acknowledgement is due also to Messrs. D. F. Lange, W. F. Wilsky and others in the Civil Engineering Department's Shop for their excellent workmanship in making specimens and maintaining the test equipment used in this program.

II. DESCRIPTION OF TEST PROGRAM

4. Materials and Specimens

The materials used in the test program consist of the following: (a) ABS Class C normalized steel (designated as CN-steel), (b) ABS Class C as-rolled steel (designated as CA-steel), and (c) A rimmed steel (designated as E-steel). All materials were received in the form of 3/4-in. thick, 6'-0 x 10'-0 plates. The chemical composition and mechanical properties of these materials are listed in Table 1.

Eleven types of small coupon specimens, designated as C-1, C-2, C-21, C-2A, C-2A1, C-2B, C-3, R-1, R-2, S-1, and S-2, were used in this test program. The letters "C", "R", and "S" denote Circular, Rectangular, and Square cross-sections respectively. The numerals following the letter denote the specimen profile: "1" indicates a constant cross-section over 2-in. gage length, "2" indicates a reduced cross-section at the mid-length of the specimen, "21" and "2A1" indicate a constant cross-section over the center 1/2-in. of the specimen, and "3" indicates a constant cross-section over the

TABLE 1. SUMMARY OF MATERIAL PROPERTIES.

(a) Tensile Test Data (Type C-1 Specimens)

Material*	Yield Stress, ksi Upper	Yield Stress, ksi Lower	Ultimate Strength, ksi	Elongation 2 in.-gage length ksi	True Fracture Stress, percent	True Fracture Strain, percent
CA (Avg. of 7 tests)	44.2	40.2	70.6	34.5	137	94
CN (Avg. of 8 tests)	48.6	46.8	68.7	35.9	143	105
E (Avg. of 4 tests)	38.3	33.5	59.3	35.6	120	98

(b) Chemical Composition - percent (check analysis)

Material*	C	Mn	P	S	Si	Cu	Cr	Ni	Al
CN and CA	0.24	0.69	0.022	0.030	0.20	0.22	0.08	0.15	0.034
E	0.21	0.34	0.019	0.030	0.01	0.18	0.12	0.19	0.003

* CN - ABS-C Normalized Steel
CA - ABS-C As-rolled Steel
E - Rimmed Steel

center 1/4-in. of the specimen. Details for all types of specimens are shown in Figs. 1, 2, and 3.

The type C-1 specimen is the standard ASTM 1/2-in. diameter tension test coupon and was used to obtain the engineering properties of the materials. The type C-2 specimen was the principal type of specimen tested. The reduced central section localized the deformation and readily permitted measurement of the minimum cross-sectional area. The type C-2 specimen has a circular

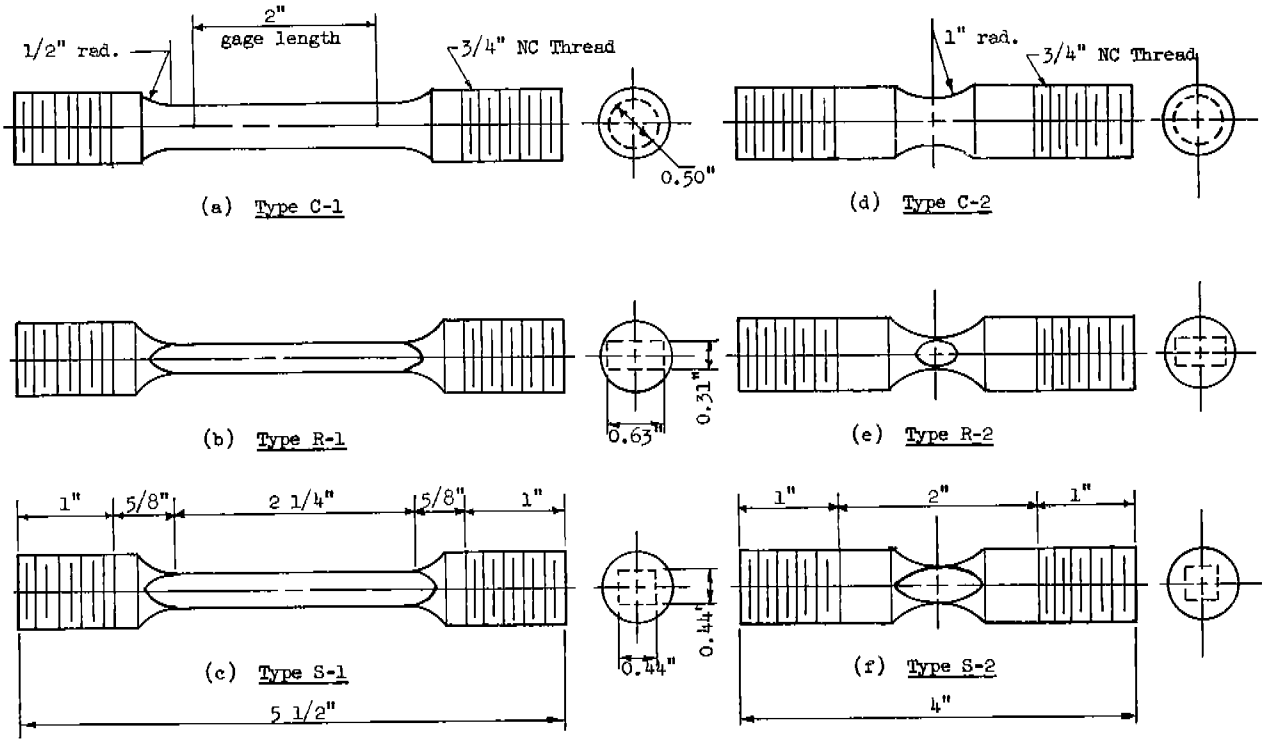

FIG. 1. DETAILS OF SERIES 1 AND 2 SPECIMENS.

curvature of 1-in. radius at the test section, while the type C-2A and C-2B specimens have corresponding radii of 1/8-in. and 3-in. respectively. The theoretical stress concentration factors for the types C-2, C-2A, and C-2B specimens are 1.10, 1.68, and 1.03 respectively. The type C-3 specimens were used only to determine the zero-to-tension s-n curve at long lives for CN-steel. Specimens with a rectangular or square cross-section were used to provide an indication of the influence of the shape of the cross-section on the low-cycle fatigue behavior.

In the initial stages of this investigation, most specimens were made with threaded ends. Later, when two specimens which had been subjected to large pre-compressive strains failed in the threaded section, specimens with flat pin ends, as shown in Fig. 3, were adapted to protect against such failures. In testing the pin ended specimens, tensile forces were transmitted

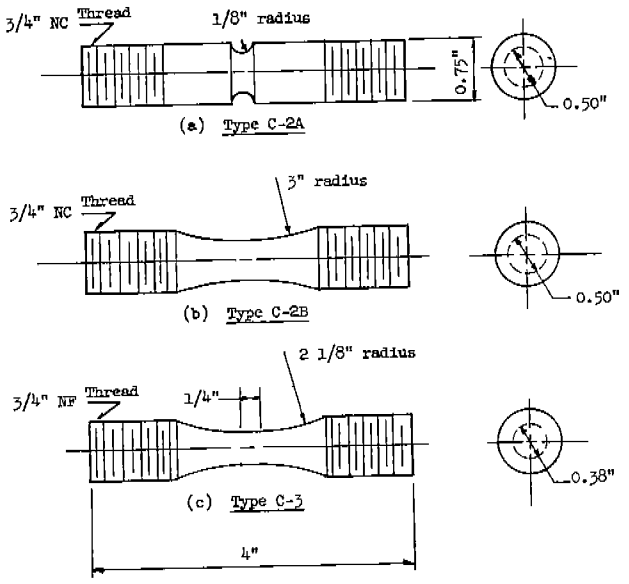

FIG. 2. DETAILS OF TYPES C-2A, C-2B AND C-3 SPECIMENS.

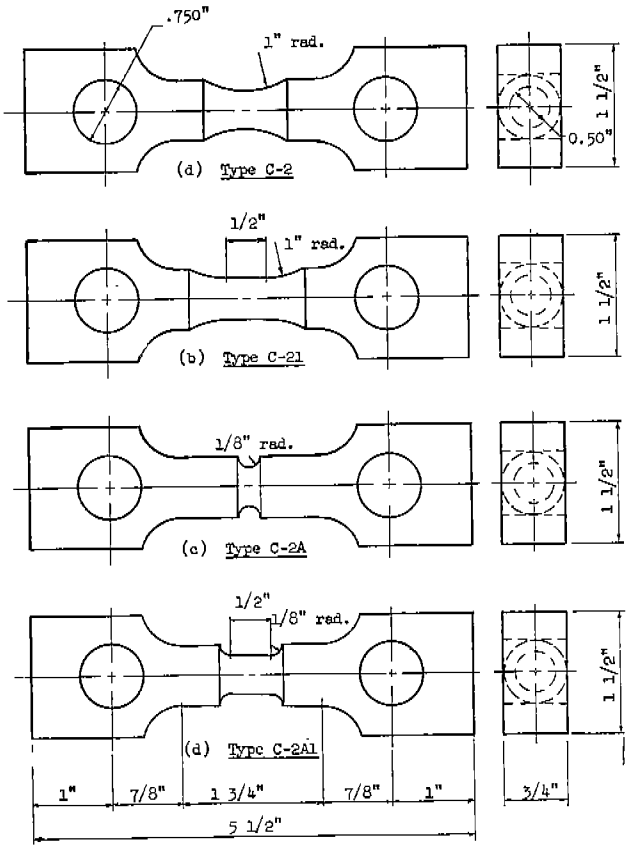

FIG. 3. DETAILS OF TYPES C-2, C-21, C-2A, AND C-2A1 SPECIMENS.

through the pin-connections and compressive forces were applied to the machined flat ends.

All specimens were polished with four grades of polishing cloth: No. 120 X metalite cloth, medium grade emery cloth, No. 320 emery cloth, and crocus cloth. In the initial period of this test program a few specimens made of CN-steel were polished in a circumferential direction. However, the remaining specimens were longitudinally polished.

5. Testing Equipment

Two hydraulically-operated universal testing machines, a 60,000-lb and a 120,000-lb testing machine, were used for static tension tests, "one-cycle" tests, part of the cyclic load tests, and most cyclic strain tests.

A 10,000-lb universal fatigue testing machine was used for the long

life zero-to-tension fatigue tests. The machine is a constant-load type in which the mean stress is applied through a static loading system. The alternating stress is obtained from the centrifugal force that is produced with an adjustable eccentric weight revolving at a constant speed of 1800 rpm.

A 50,000-lb Illinois lever-type fatigue testing machine, see Fig. 4, was used for the reversed load fatigue tests. A set of special reversed-load

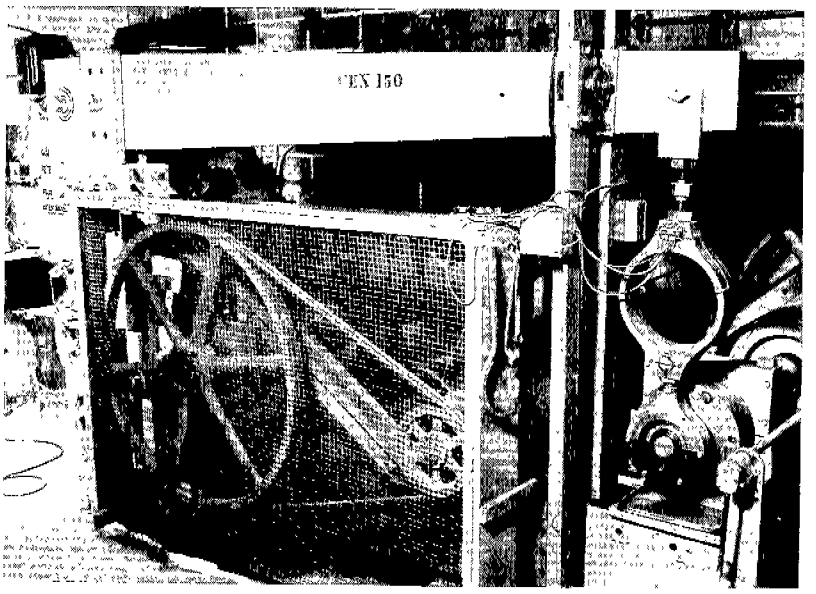

FIG. 4. 50,000-POUND ILLINOIS-TYPE FATIGUE TESTING MACHINE.

pull-heads were used to transmit the loads to the test specimens. These heads, shown in Figs. 5 and 6, transmit tensile forces through pin-connections and compression through bearing on wedging compression blocks, which bear on the flat ends of the specimen.

An optical device was used to obtain the initial diameter of the test specimens. To measure the diameter of the specimens during the tests, several small diameter-measuring devices were used. In the static tests dial-type diameter gages were used. For the fatigue tests a special diameter gage was fabricated with SR-4 strain gages to provide a measure of the changes in specimen diameter. The output of these gages was linearly proportional to the diameter change and provided a strain increment of one microinch per inch for

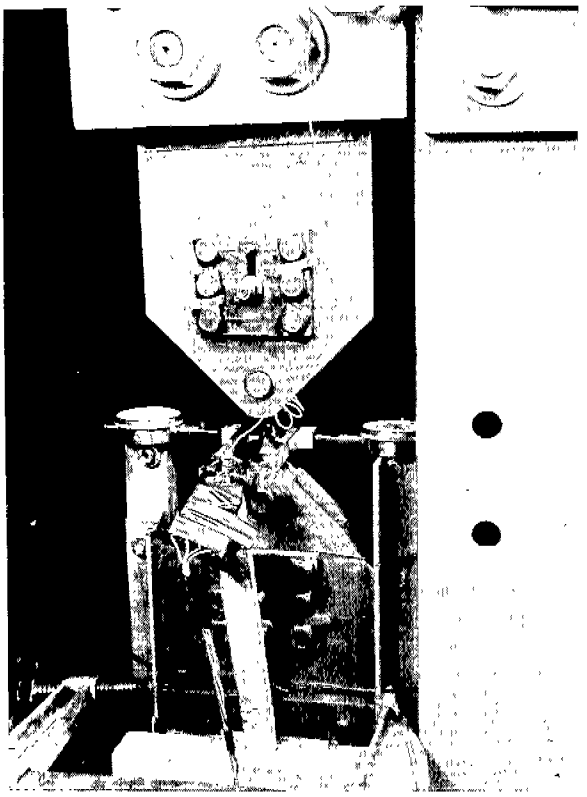

FIG. 5. REVERSED-LOAD PULL-HEADS WITH A TEST SPECIMEN IN POSITION.

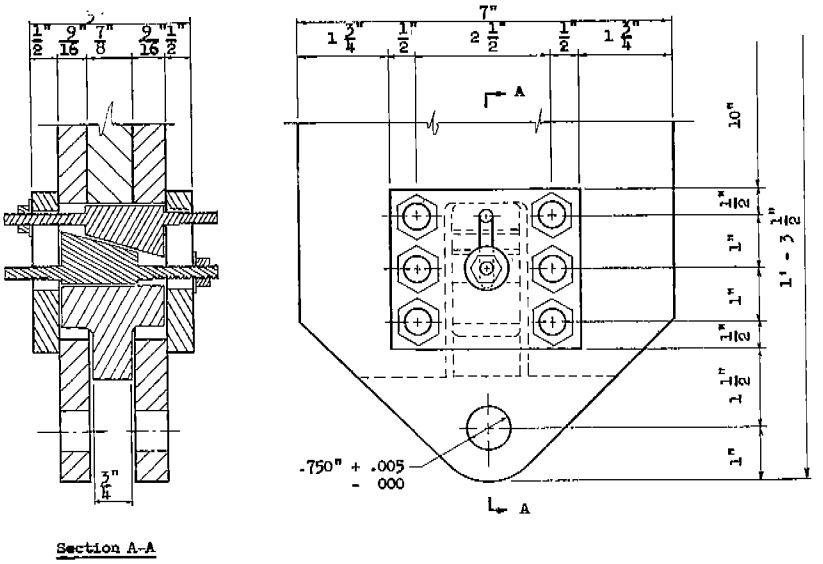

FIG. 6. DETAILS OF THE REVERSED-LOAD PULL-HEAD.

each 0.00016 in. change in specimen diameter. Special recorders were used to record simultaneously the variation of specimen diameter, the load, and the duration of the tests.

6. Description of Tests and Test Procedures

A. One-Cycle Tests

If the fatigue life is defined as the number of tensile load applications to failure, the lowest possible number of cycles in any fatigue tests is "one." In the zero-to-tension fatigue tests, the "one-cycle" tests is a static tension test and, similarly, in reversed-load fatigue tests the "one-cycle" test is simply a tension test of specimens that have been pre-compressed. In the present report, these are all referred to as "one-cycle" tests.

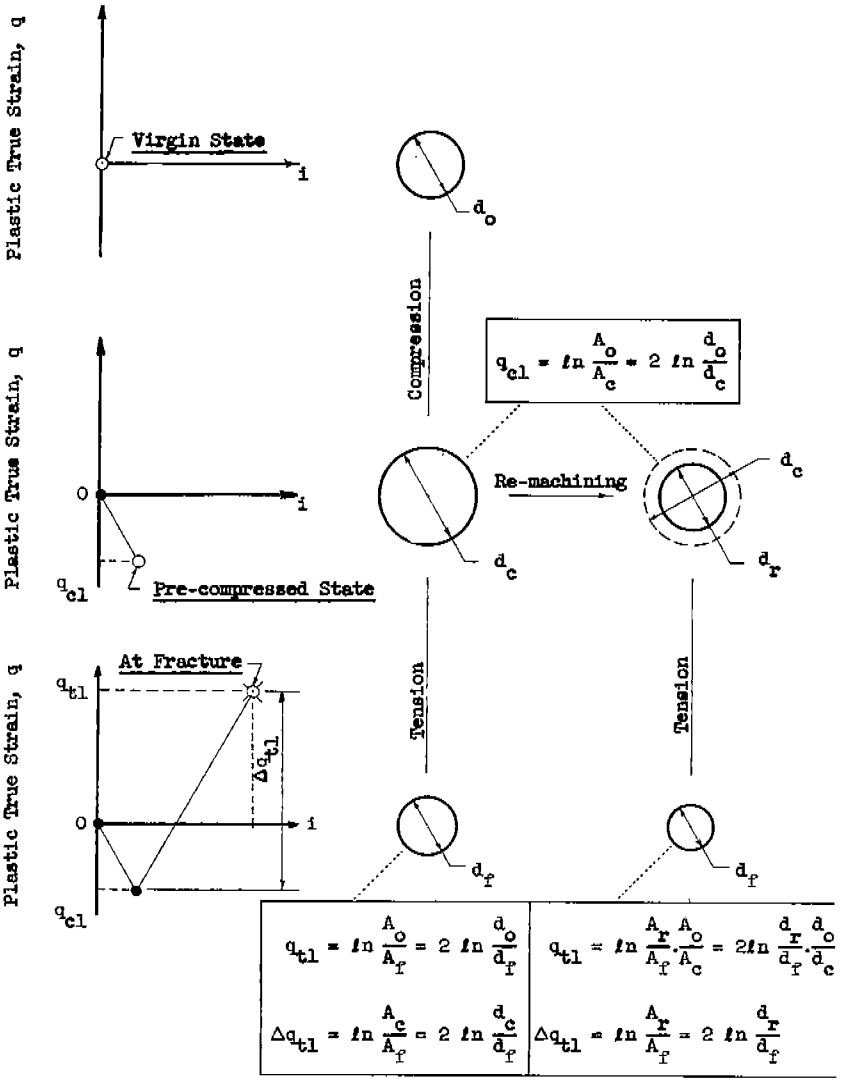

FIG. 7. STRAIN-CALCULATION PROCEDURE FOR "ONE-CYCLE" TEST

In the early stages of the investigation it was found desirable to evaluate the data in terms of the true strain. To obtain such data for "one-cycle" tests the strain calculation procedure illustrated in Fig. 7 was used. In the virgin state, the test section had an original diameter of d_o and a plastic true strain of zero. After a plastic compressive loading the test section was enlarged and possessed a new diameter, d_c, and a corresponding plastic true strain of q_{cl}. At this stage, some of the specimens were re-machined to their original size and shape. These specimens with a new diameter, d_r, are assumed to possess a plastic pre-strain of q_{cl}. The specimens, either in the as-compressed or in the re-machined condition, were then loaded in tension to fracture. The specimen diameter at the fractured section, d_f, was used for the computation of the plastic true strain at fracture, q_{tl}, and the tensile change in plastic true strain, Δq_{tl}.

The true strain, q, as presented by MacGregor[3] may be computed from area measurements by the following relationship,

$$q = -\int_{A_o}^{A} \frac{dA}{A} = \ell n \frac{A_o}{A} \qquad (1)$$

where A_o and A are respectively the original and the instantaneous areas of the specimen. By definition, true strain refers to a localized deformation over a given cross section while engineering strain represents an average of the gross deformation over a given length. Since failure in low-cycle fatigue is generally a localized phenomenon, the true strain is considered to be a better representation of the plastic deformation at the critical section than the engineering strain and will be used in this study.

After a specimen has been pre-compressed the plastic true pre-compressive strain, from Eq. (1) will be,

$$q_{cl} = \ell n \frac{A_o}{A_c} = 2 \ell n \frac{d_o}{d_c} \qquad (2)$$

Then, if the specimen is loaded in tension to fracture, the plastic true strain at fracture is found to be,

$$q_{tl} = \ell n \frac{A_o}{A_f} = 2 \ell n \frac{d_o}{d_f} \qquad (3)$$

and the tensile change in plastic true strain,

$$\Delta q_{tl} = \ell n \frac{A_c}{A_f} = 2 \ell n \frac{d_c}{d_f} \qquad (4)$$

When a re-machined specimen is used for this purpose the corresponding relationships will be,

$$q_{tl} = \ell n \frac{A_r}{A_f} \cdot \frac{A_o}{A_c} = 2 \ell n \frac{d_r}{d_f} \cdot \frac{d_o}{d_c} \qquad (5)$$

and

$$\Delta q_{tl} = \ell n \frac{A_r}{A_f} = 2 \ell n \frac{d_r}{d_f} \qquad (6)$$

All "one-cycle" tests were conducted on type C-2 specimens. To prevent buckling of the test section at the extremely high compressive loads, a special "sleeve and slide" assembly was used. The specimen was tested by (a) inserting short steel pins into the pin-holes at both ends of the specimen to prevent excessive deformation of the holes, (b) placing the specimen at the center of the "slide" blocks, with small copper shims filling the space between the specimen heads and the inside wall of the "slide" blocks, and (c) fitting the assembly into the "sleeve" and then loading to the desired deformation. A picture of a specimen in the "slide" blocks and the "sleeve" is shown in Fig. 8. The entire assembly was then centered in the testing machine and a dial-type diameter gage set in a position to measure the diameter of the specimen at mid-length. This measurement would be approximate because the material is

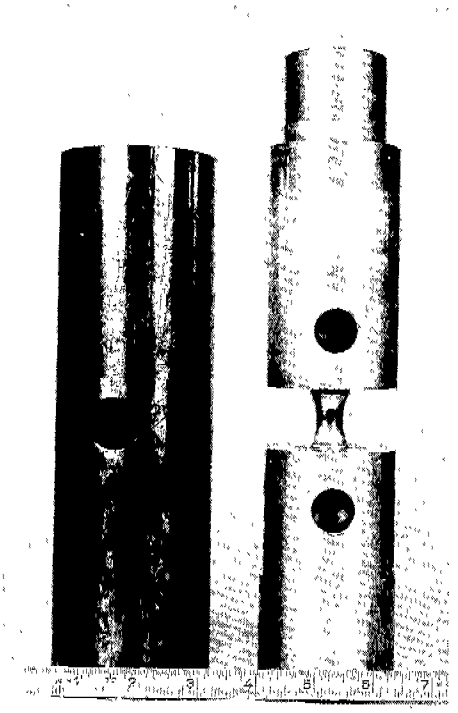

FIG. 8. "SLEEVE AND SLIDE" ASSEMBLY.

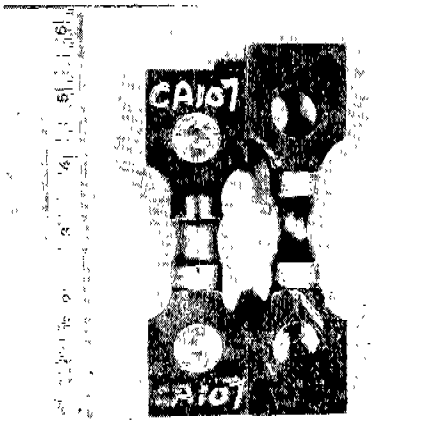

FIG. 9. TYPICAL PRE-COMPRESSED SPECIMEN SHOWN ON THE LEFT OF A VIRGIN SPECIMEN.

not isotropic and the plastically deformed test section may not remain perfectly circular in shape. However, when the specimen was removed from the "sleeve and slide" assembly, the diameter of the specimen was again measured in two perpendicular directions with the optical diameter-measuring device and the average of these measurements was used as the basis for the plastic true strain computations.

In general, the specimens remained relatively straight and true during the pre-compression loading. A typical pre-compressed specimen (q_{cl} = 51%) is shown in Fig. 9 along with a virgin specimen. After the specimens were plastically pre-compressed to various degrees, the short pins were removed from the pin-holes of the specimens and the holes reamed with a 3/4-in. standard reamer. The re-machined specimens were then re-processed in the same manner as the original specimens. The subsequent tension tests were conducted using the "slide" blocks as pull-heads. After the specimen failed, the diameter at the fractured section was again measured with the optical diameter-measuring device to determine the tensile change in plastic true strain.

B. Cyclic Load Tests

In the cyclic "load" tests, the load limits in every cycle were maintained constant throughout the test. When the specimen could no longer carry the required maximum load in the test, the specimen was considered to have "failed." Approximately 100 specimens were tested in this manner at two stress ratios, i.e., $R_s = 0$ and -1, the stress ratio, R_s, being defined as the ratio between the cyclic minimum engineering stress and the cyclic maximum engineering stress.

All low-cycle constant load fatigue tests on a zero stress ratio, i.e., zero-to-tension, were carried out in a 120,000-lb universal testing machine. For the series 1 specimens a continuous record of load and elongation, as shown in Fig. 10, was obtained using a 2-in. gage-length extensometer. However, for most of the series 2 specimens, a record of the changes of diameter of the minimum section was obtained with the special diameter gage.

In several of the tests of type C-2 and C-2A specimens the load was adjusted and maintained at a level slightly less than the usual ultimate strength. This load was maintained until the specimen was deformed to such an extent that it could no longer carry the load. A record for such a test is shown in Fig. 11. A few type C-2 and C-2A specimens were also subjected to intermittently sustained cycles of load, the periodic loading and unloading cycles being patterned so that the time at maximum load remained constant for each cycle during the life of a particular specimen. A typical record of the load and the change in diameter with respect to time, for one of these tests, is shown in Fig. 12. The type C-3 specimens were tested at a speed of 1800 cycles per minute to obtain a conventional long-life zero-to-tension s-n curve for the CN-steel.

The cyclic "load" tests in reversal and at extremely high stresses were conducted in a 60,000-lb universal testing machine with a test procedure similar to that described previously for the "one-cycle" tests. In some cases,

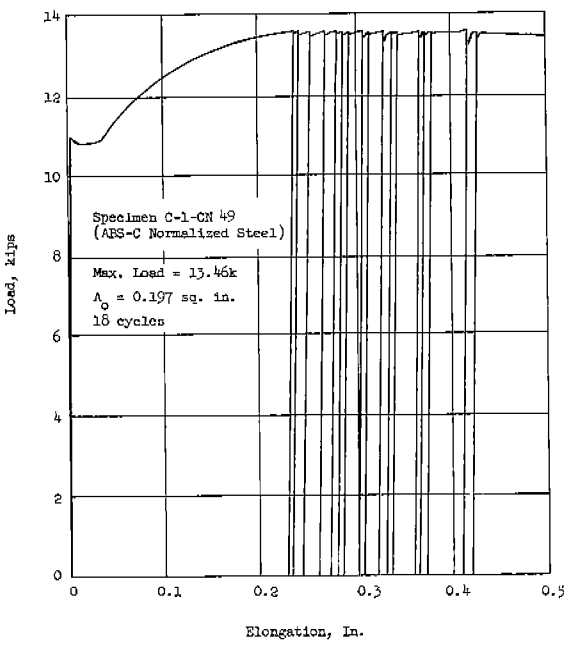

FIG. 10. A TYPICAL RECORD OF LOAD VS. ELONGATION FOR A TYPE C-1 SPECIMEN SUBJECTED TO REPEATED CONSTANT TENSILE LOADS.

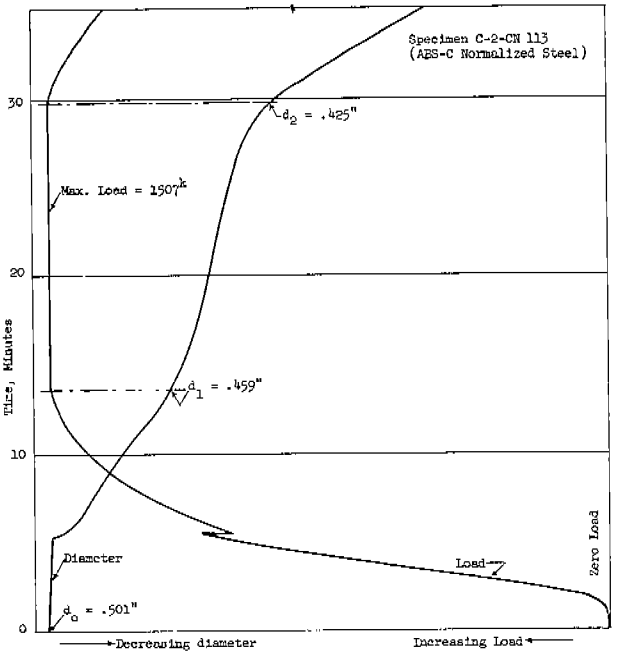

FIG. 11. LOAD-DIAMETER-TIME RECORD FOR A TYPE C-2 SPECIMEN SUBJECTED TO SUSTAINED MAXIMUM TENSILE LOAD.

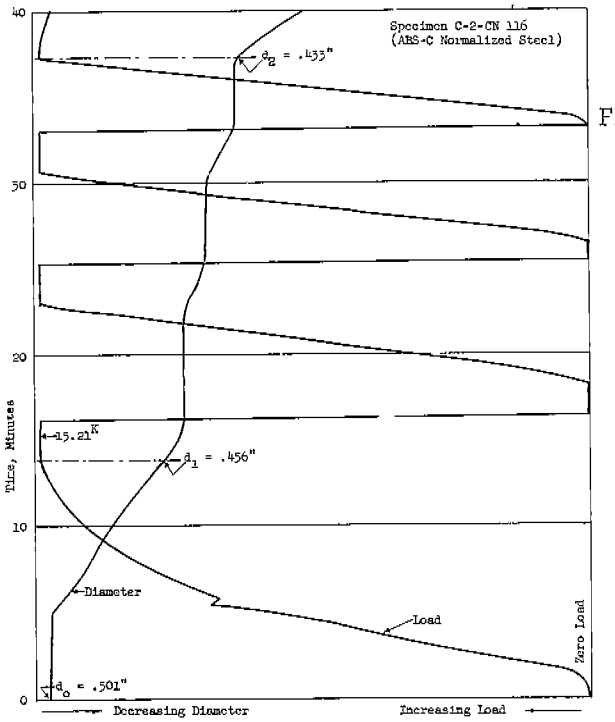

FIG. 12. LOAD-DIAMETER-TIME RECORD FOR A TYPE C-2 SPECIMEN IN A SLOW ZERO-TO-TENSION FATIQUE TEST

the specimens were tested with the first load applied in compression and in other cases with the first load applied in tension. The specimens were then subsequently subjected to constant alternating loads until failure occurred. Measurements were taken of the specimen diameter after each loading to determine the corresponding change in strain.

Thirty-four specimens (Type C-2, C-21, C-2A and C-2A1) were tested under reversed-load in the Illinois-type fatigue testing machine. After a specimen was placed in the machine, the desired load limits were set and the load was applied manually for the first 10 cycles or until the load limits were stabilized. The machine was then run at a cyclic rate of 40 rpm. However, at short intervals, the machine was stopped and the load checked and readjusted when necessary. During the tests, a magnifying glass was used to establish and observe the initiation of the fatigue cracks. In general, several cracks were found to develop at about the same time. These cracks then propagated slowly until some of them merged to form a larger crack. Therefore, the fractures often exhibited a zig-zag or step appearance at failure.

C. Cyclic Deformation Tests

To study the effect of cyclic compressive deformation on low-cycle fatigue behavior, cyclic strain tests were conducted at constant values of relative-strain ratio, defined as the ratio of the cyclic compressive change in plastic deformation to the subsequent tensile change in plastic deformation. A relative-strain ratio may be expressed in terms of engineering strain or true strain, as follows,

$$r_{\epsilon} = \frac{\Delta\epsilon_c}{\Delta\epsilon_t} \tag{7}$$

$$r_q = \frac{\Delta q_c}{\Delta q_t} \tag{8}$$

Cyclic strain tests were conducted at constant relative-strain ratios of -1/4, -1/2, -3/4 and -1. The corresponding strain cycles are illustrated in Fig. 13 where only the limiting values of plastic true strain

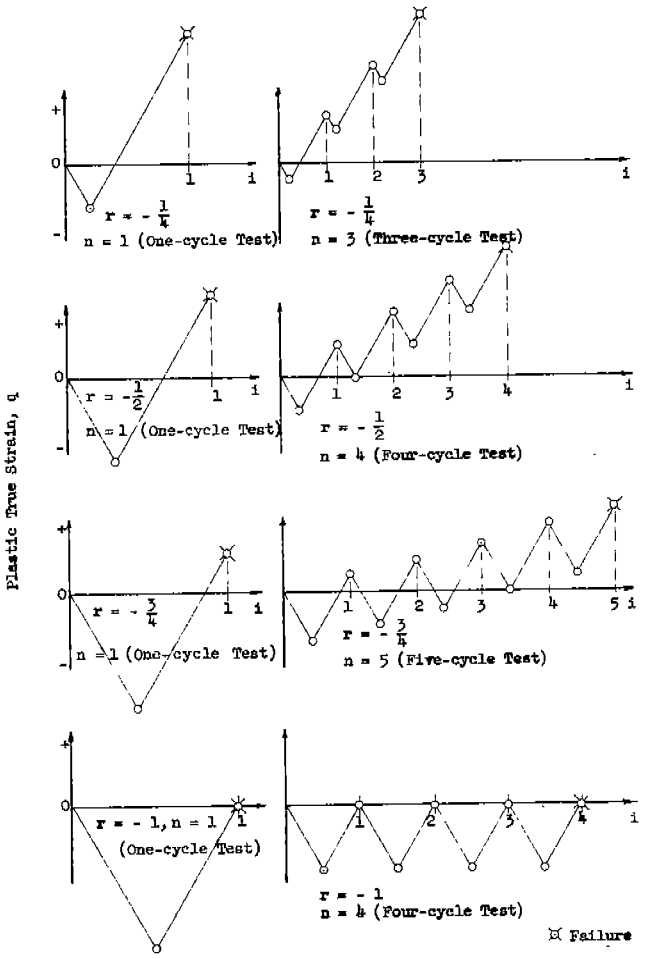

FIG. 13. CYCLIC STRAIN TESTS AT VARIOUS RELATIVE-STRAIN RATIOS

at the maximum tensile and compressive load applications are presented. Prior to the start of a test the desired limits of diameter for each cycle were predetermined from a given combination of r and Δq_t. The tests were then conducted with a procedure similar to that used for the "one-cycle" tests.

A number of the specimens subjected to the lower strain ranges and at a relative strain ratio of -1 were tested in the Illinois fatigue testing machine. In these tests, the special diameter gage was mounted on the minimum section of the specimen throughout the test. The electrical output of the

gages and that of the load dynamometer of the fatigue machine were respectively recorded on an X-Y recorder. The fatigue machine was manually controlled to apply either tension or compression. When the change in the specimen diameter approached the selected value, Δd, the machine was stopped and run in the reverse direction until the specimen diameter was reduced to a value close to the original diameter, d_o. The specimen was cycled in this manner between diameter limits of d_o and $d_o + \Delta d$ until the specimen fractured. A typical stress-diameter diagram is shown in Fig. 14. Due to the inertia of the testing machine, the change in material properties, and the effect of the elastic recovery of the specimen, it was difficult to cycle the specimens within precise diametrical limits. Nevertheless, it was found that the change in diameter varied no more than a few percent from the desired value.

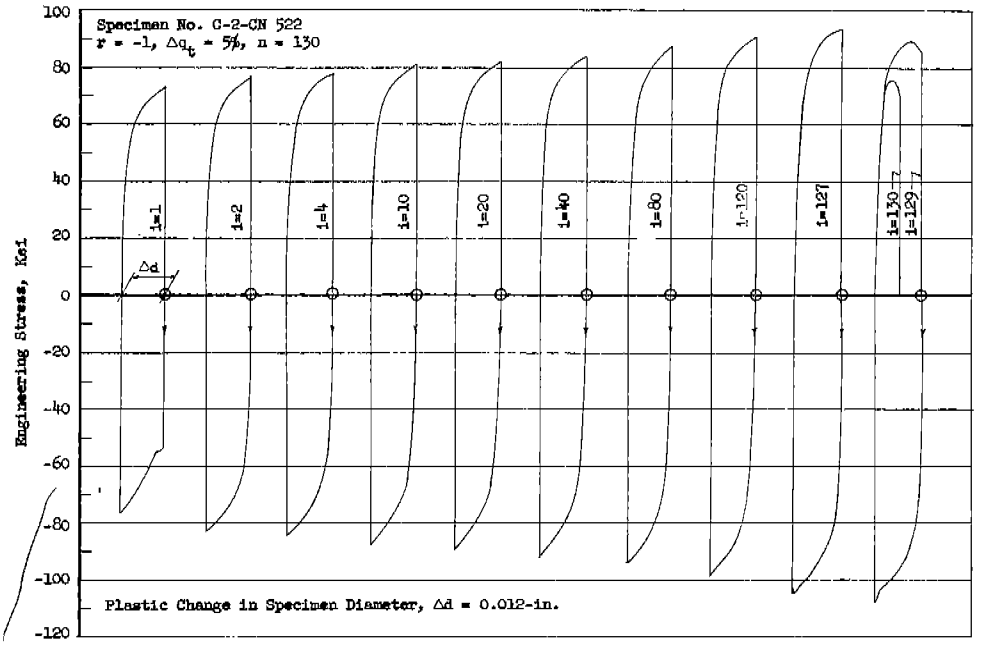

FIG. 14. TYPICAL STRESS VS. DIAMETER DIAGRAMS.

III. DESCRIPTION AND ANALYSIS OF TEST RESULTS

7. One-Cycle Tests

The results of all one-cycle tests are presented in Table 2 in terms of engineering stress, true stress, and true strain. Some of the specimens, it may be noted, were re-machined after the compressive loading while others were not. Nevertheless, there does not appear to be any significant difference in the results obtained from the two types of specimens.

In the one-cycle tests with no pre-compression, i.e., simple tension tests, true stress-true strain diagrams were obtained for specimens of CN, CA, and E steels and are shown respectively in Figs. 15, 16, and 17. It may be seen that the curves for both C-steels are similar although the CA steel specimens failed at a lower strain value than the CN-steels specimens. The σ-q curve for E-steel lies below the other two curves by a considerable amount. However, the plastic true strain at fracture for the E-steel specimens was slightly greater than that for the CA-steel and about the same as that for the CN-steel.

The "one-cycle" variation of tensile change in plastic true strain, Δq_{t1}, with respect to the plastic true pre-compressive strain, q_{c1}, is plotted in Figs. 18, 19, 20 and 21 respectively for types C-2 and C-2A specimens of CN-steel, type C-2 specimens of CA-steel and type C-2 specimens of E-steel. In Figs. 22, these data, in terms of true strains, are all summarized and plotted together in normalized form. It appears that in general Δq_{t1}, the tensile change in true plastic strain at n = 1, decreases with an increase in pre-compression. However, the effect of the pre-compression on the tensile change in plastic strain is not the same for the different materials. At the smaller values of pre-strain the specimens of CA and CN-steel exhibited little change in the tensile change in true plastic strain while the E-steel specimens gave a continual decrease with an increase in the pre-compression. Nevertheless, at pre-compression strains greater than about 40 percent the rate

TABLE 2. SUMMARY OF "ONE-CYCLE" TESTS

Specimen No.	Re-Machined	Engineering Stress, ksi		True Stress, ksi		True Strain, percent		
		Maximum Compression	Tension (At Fracture)	Maximum Compression Load	Tension (At Fracture)	Compression	At Fracture	
		s_c	s_u	σ_c	σ_f	q_{cl}	q_{tl}	Δq_{tl}
C-2-CN3	No	0	76	0	146	0	85	85
C-2-CN15	No	0	77	0	144	0	86	86
C-2-CN29	No	0	76	0	139	0	86	86
C-2-CN30	No	0	76	0	146	0	88	88
C-2-CN64	No	0	77	0	132	0	83	83
C-2-CN114	No	0	76	0	143	0	84	84
C-2-CN123	No	-69	82	-66	144	-5	82	87
C-2-CN140*	No	-70	79	-70	142	-6	78	84
C-2-CN120	No	-84	83	-78	143	-8	77	85
C-2-CN119	No	-99	88	-88	142	-12	72	84
C-2-CN134*	Yes	-100	90	-89	140	-12	71	83
C-2-CN126*	No	-99	90	-88	143	-12	72	84
C-2-CN128*	Yes	-118	104	-97	144	-20	65	85
C-2-CN125*	No	-119	105	-96	142	-21	63	84
C-2-CN121	No	-127	109	-99	145	-25	62	87
C-2-CN118	No	-139	116	-104	146	-29	55	84
C-2-CN139*	No	-137	119	-102	146	-30	54	84
C-2-CN136*	Yes	-139	121	-103	144	-30	53	83
C-2-CN127*	Yes	-158	139	-107	149	-40	44	84
C-2-CN137*	Yes	-172	150	-109	154	-46	40	86
C-2-CN129	Yes	-188	155	-117	148	-48	29	77
C-2-CN523	Yes	-201	168	-117	157	-54	27	81
C-2-CN122	No	-162	127		Failed in Threads			
C-2A-CN156	No	0	96	0	157	0	60	60
C-2A-CN303	No	-77	98	-75	152	-2	57	59
C-2A-CN304	No	-100	101	-95	157	-6	57	63
C-2A-CN307	No	-128	112	-113	149	-13	44	57
C-2A-CN309	No	-144	121	-121	140	-17	28	45
C-2A-CN305	No	-150	124		Failed in Threads			
C-2-CA2	No	0	79	0	140	0	77	77
C-2-CA10	No	0	78	0	144	0	77	77
C-2-CA101	No	0	79	0	138	0	76	76
C-2-CA109	No	0	78	0	140	0	78	78
C-2-CA111	No	-92	87	-84	141	-9	70	79
C-2-CA11	No	-117	102	-97	144	-19	61	80
C-2-CA106	Yes	-130	114	-101	146	-25	56	81
C-2-CA6	No	-141	121	-105	145	-30	47	77
C-2-CA15	No	-159	134	-109	145	-38	37	75
C-2-CA114	Yes	-155	135	-107	147	-40	38	78
C-2-CA107	Yes	-189	163	-113	150	-51	23	74
C-2-CA105	Yes	-216	179	-119	151	-59	10	69
C-2-E2	No	0	64	0	123	0	82	82
C-2-E10	No	0	64	0	124	0	85	85
C-2-E101	No	0	65	0	125	0	85	85
C-2-E109	No	0	62	0	125	0	95	95
C-2-E14	No	-80	76	-72	118	-11	63	74
C-2-E103	No	-102	88	-83	124	-21	60	81
C-2-E8	No	-126	107	-92	127	-31	47	78
C-2-E113	Yes	-142	122	-95	129	-40	36	76
C-2-E11	No	-142	122	-95	134	-40	34	74
C-2-E12	No	-169	141	-101	125	-52	20	72
C-2-E115	Yes	-169	141	-104	132	-49	20	69
C-2-E116	Yes	-202	168	-107	134	-63	4	67

*The specimen was artificially aged at 150°C for 90 minutes before the tensile test.

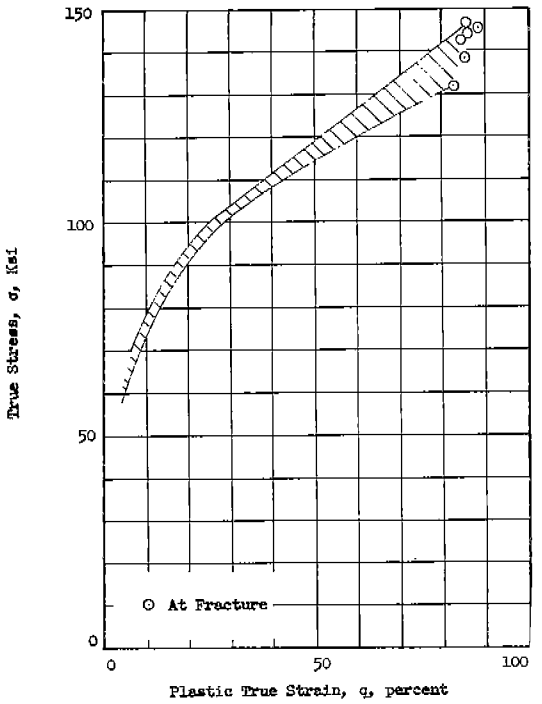

FIG. 15. TRUE STRESS VS. TRUE STRAIN RELATIONSHIP FOR TYPE C-2 SPECIMENS OF ABS-C NORMALIZED (CN) STEEL IN SIMPLE TENSION

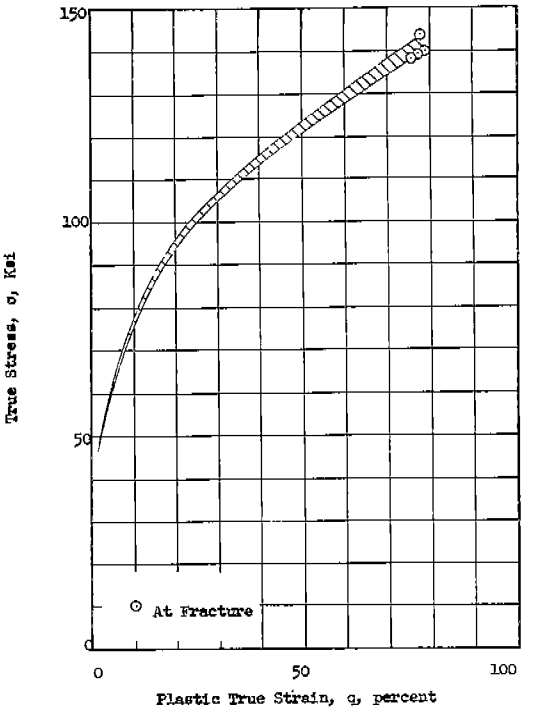

FIG. 16. SAME AS FIG. 15. FOR TYPE C-2 SPECIMENS OF ABS-C AS-ROLLED (CA) STEEL IN SIMPLE TENSION.

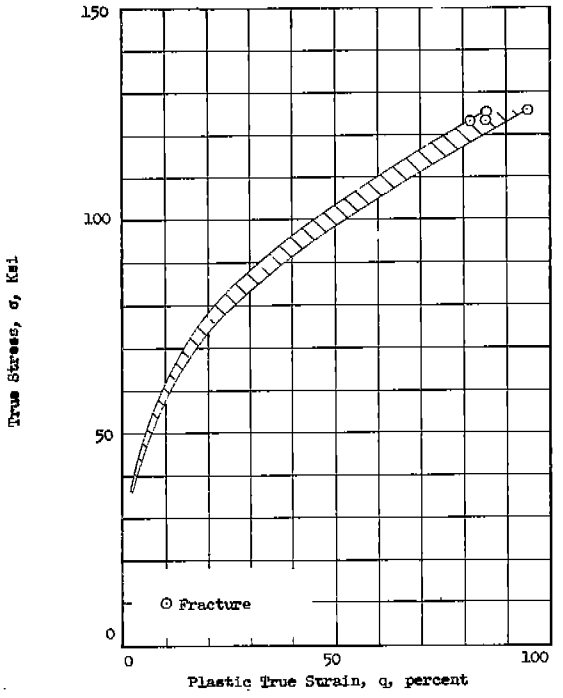

FIG. 17. TRUE STRESS VS. TRUE STRAIN RELATIONSHIP FOR TYPE C-2 SPECIMENS OF RIMMED (E) STEEL IN SIMPLE TENSION.

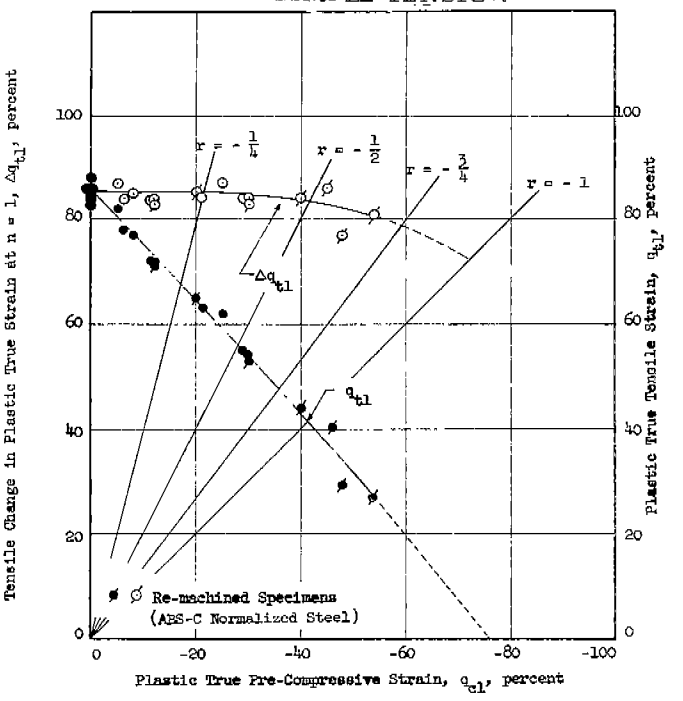

FIG. 18. TYPE C-2 SPECIMENS OF ABS-C NORMALIZED (CN) STEEL.

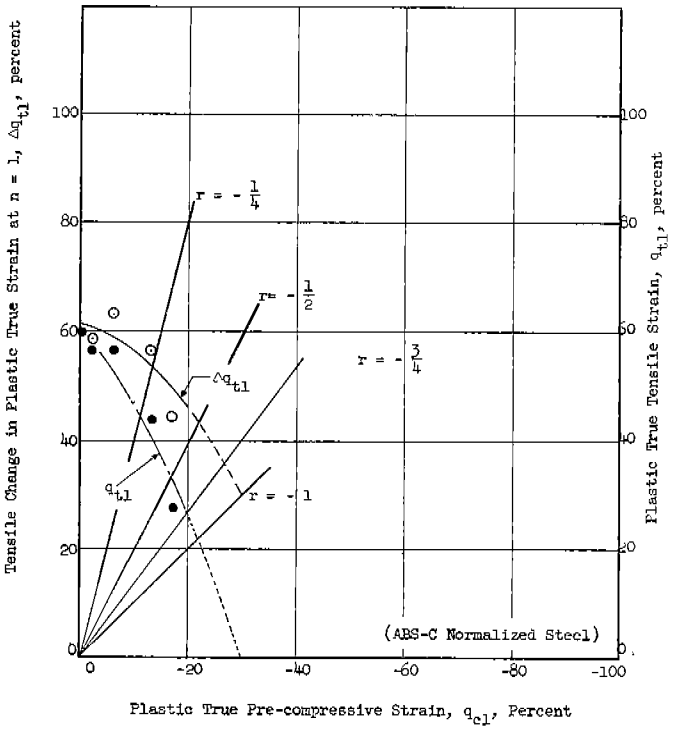

FIG. 19. TENSILE CHANGE IN PLASTIC TRUE STRAIN AND PLASTIC TRUE TENSILE STRAIN AT FRACTURE VS. PLASTIC TRUE PRE-COMPRESSIVE STRAIN FOR TYPE C-2A SPECIMENS OF ABC-C NORMALIZED (CN) STEEL.

of change of Δq_{tl} was approximately the same for all three steels. In the figures it is evident that the total plastic strain necessary to cause fracture after a compressive pre-straining will be a function not only of the pre-compression but also a function of the material. Furthermore, the figures

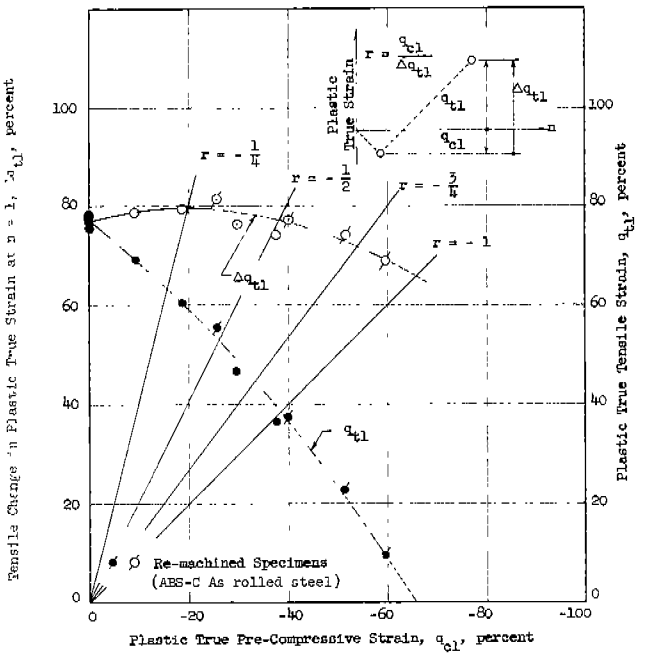

FIG. 20. TENSILE CHANGE IN PLASTIC TRUE STRAIN AND PLASTIC TRUE STRAIN AT FRACTURE VS. PLASTIC TRUE PRE-COMPRESSIVE STRAIN FOR TYPE C-2 SPECIMENS OF ABS-C AS-ROLLED (CA) STEEL.

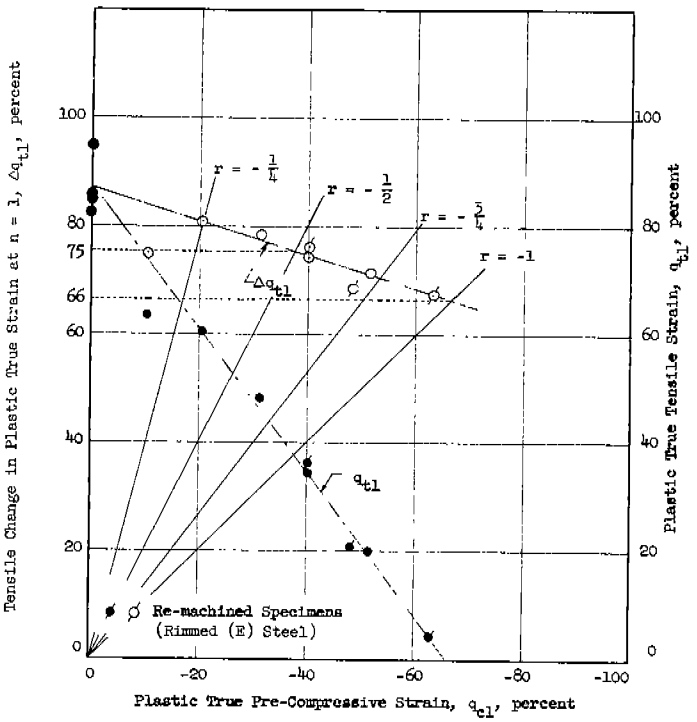

FIG. 21. TENSILE CHANGE IN PLASTIC TRUE STRAIN AND PLASTIC TRUE STRAIN AT FRACTURE VS. PLASTIC TRUE PRE-COMPRESSIVE STRAIN FOR TYPE C-2 SPECIMENS OF RIMMED (E) STEEL.

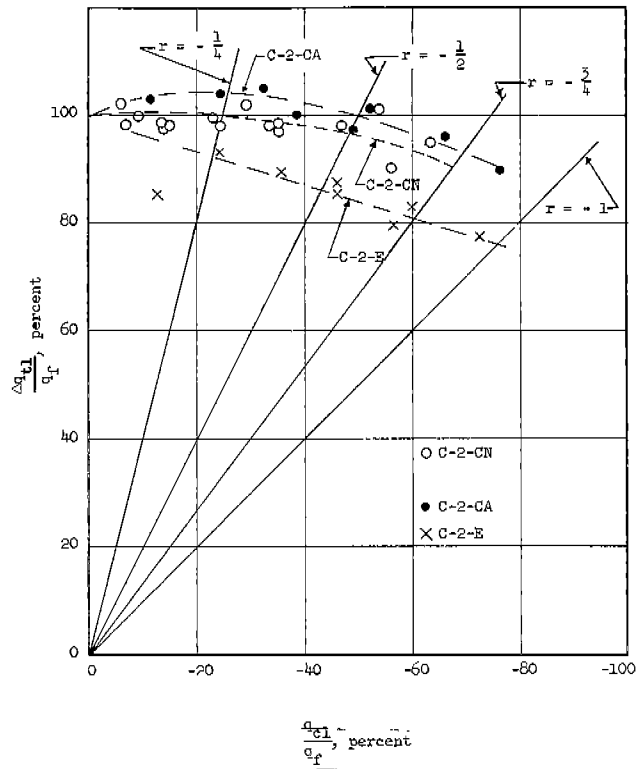

FIG. 22. NORMALIZED RELATIONSHIPS FOR TENSILE IN PLASTIC TRUE STRAIN VS. PLASTIC TRUE PRE-COM-PRESSIVE STRAIN.

demonstrate that, although the plastic true tensile strain q_{tl}, based on the original dimensions of the specimens, decreased markedly with the magnitude of

the pre-compression, the total change, Δq_{t1}, did not vary significantly for pre-strains as high as 40 percent.

From an examination of Figs. 18 and 19 it may be seen that the geometry of the specimen may also have a marked effect on the relationship between the pre-compression and tensile strain to failure. The type C-2A specimen with a small (1/8 in.) radius failed at much smaller plastic true strain than did the type C-2 specimens with a 1-in. radius.

The one-cycle test data may also be considered in terms of engineering stresses, as shown in Fig. 23. Here it is found that the pre-compression affects the ultimate tensile strength when the pre-compressive stress exceeds the basic tensile strength of the material. However, it must be remembered that the area changes as a result of the plastic deformation in pre-compression and affects markedly this relationship.

8. Cyclic Load Tests

Zero-to-Tension Tests. All low-life specimens subjected to zero-to-tension loadings (constant maximum load) were tested with very high loads in a manually operated universal testing machine. The cyclic rate for most tests

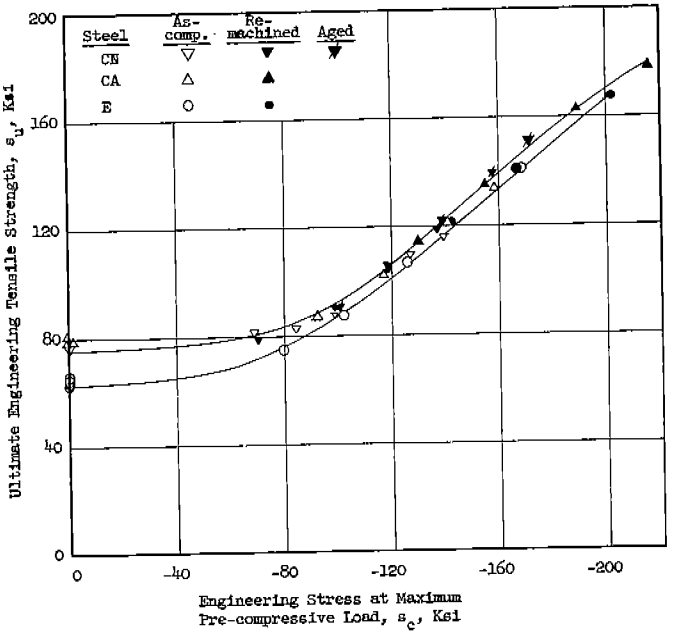

FIG. 23. VARIATION OF ULTIMATE TENSILE STRENGTH OF TYPE C-2 SPECIMENS WITH CORRESPONDING ENGINEERING STRESS AT MAXIMUM PRE-COMPRESSIVE LOAD.

was approximately one cycle per minute. The C-3 specimens (used for long life tests) were tested in a Sonntag fatigue testing machine at a speed of 1800 cpm. The results of these zero-to-tension fatigue tests are listed in Table 3.

A complete s-n curve for unnotched specimens (types C-1 and C-3) of CN-steel is shown in Fig. 24. It is to be noted that type C-1 specimens were tested at a speed of 1 cpm while type C-3 specimens were tested at a speed of 1800 cpm. Nevertheless, this diagram serves to indicate the general zero-to-tension fatigue behavior for the CN-steel and provides a fatigue limit for this material of approximately 52,500 psi at a life of between 10^6 and 10^7 cycles.

Conventional s-n curves for series 1 and 2 specimens of CN-steel were also obtained and are shown in Fig. 25 for lives of less than 1,000 cycles. It is found that there was no significant difference in behavior for the various cross-sectional shapes (round, square or rectangular). However, a reduction in the radius at the test section, although providing an increase in theoretical stress concentration, provided also an increase in the fatigue resistance of the members at the short lives. This effect is just the opposite of that which a notch produces in the fatigue strength at longer lives. Again, it is seen that the geometry of the specimens (that producing a stress concentration) has an effect on their behavior.

A further evaluation of the low-cycle fatigue data, based on the true stresses at the first as well as the last maximum load is presented in Fig. 26 along with the relationship for the maximum engineering stress for type C-2 specimens. The divergence of the true stress curve in this diagram illustrates that during the tests there was more change in the cross-sectional area of the test specimens subjected to the lower loads (longer lives) than in the specimens subjected to the higher loads, a condition that is generally not expected in fatigue. It must be remembered, however, that this behavior is for lives only up to approximately 400 cycles. Under long-life low-stress conditions the true stress curves can be expected to converge to the engineering stress curve. Thus,

TABLE 3. SUMMARY OF ZERO-TO-TENSION LOAD FATIGUE TEST DATA

Specimen No.	Maximum Engineering Stress, ksi, s	Cycles to Failure, n	Strain at First Max. Load, %
C-1-CN1	68.5	1	20.0
C-1-CN31	68.4	1	20.0
C-1-CN43	64.1	632	8.3
C-1-CN49	68.4	18	12.0
C-2-CN29	75.9	1	25.5
C-2-CN33	72.9	75	12.5
C-2-CN58	76.0	18	17.5
C-2-CN59	74.6	53	14.5
C-2-CN103	79.4	5	17.2
C-2-CN104	78.5	10	15.0
C-2-CN105	75.0	96	10.2
C-2-CN106	75.8	84	10.2
C-2-CN107	79.3	3	24.0
C-2-CN108	70.7	352	8.5
C-2A-CN156	95.5	1	22.0
C-2A-CN157	95.0	1	20.0
C-2A-CN158	93.8	31	12.0
C-2A-CN159	95.6	10	16.0
C-2A-CN170	91.0	55	10.5
C-2B-CN160	71.9	1	22.0
C-2B-CN161	74.5	7	17.0
C-2B-CN162	73.0	27	14.0
C-3-CN142	50.0	10,088,000*	
C-3-CN143	52.0	10,000,000*	
C-3-CN145	59.0	4,000	
C-3-CN147	53.0	2,713,000	Tested at 1800 cpm in
C-3-CN148	60.0	8,000	Fatigue Testing
C-3-CN149	58.0	328,000	
C-3-CN150	56.0	750,000	Machine (*No Failure)
C-3-CN151	54.0	497,000	
C-3-CN152	57.0	257,000	
C-3-CN154	52.5	10,547,000*	
C-3-CN155	52.8	6,504,000	
R-1-CN8	69.4	20	15.5
R-1-CN26	68.8	41	11.2
R-1-CN50	67.7	7	16.6
R-1-CN62	68.9	1	20.0
R-2-CN4	77.8	1	23.6
R-2-CN6	77.3	10	16.7
R-2-CN10	76.0	45	11.4
R-2-CN16	74.2	92	9.0
S-1-CN32	67.9	4	18.0
S-1-CN44	70.0	1	20.0
S-1-CN56	68.7	22	14.2
S-2-CN5	75.5	34	13.0
S-2-CN11	74.9	60	12.0
S-2-CN17	76.5	1	25.5
S-2-CN18	76.3	25	13.5
S-2-CN46	73.0	146	9.5
S-2-CN47	78.5	5	18.3
S-2-CN48	78.5	4	19.3

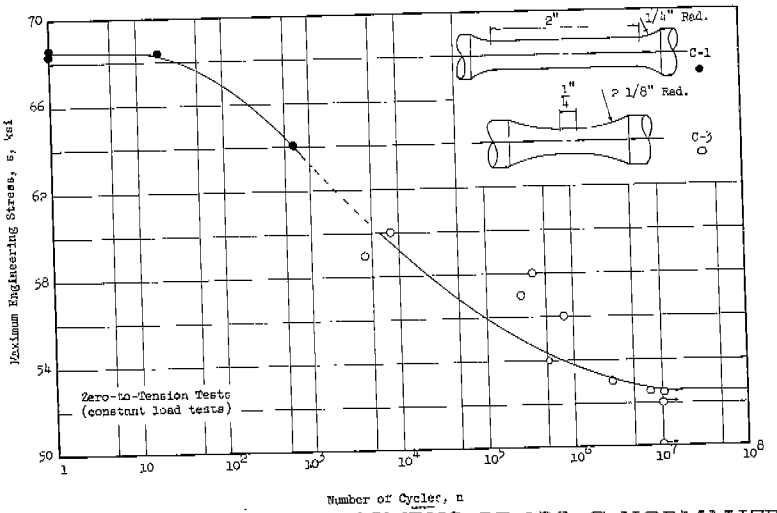

FIG. 24. S-N CURVE FOR UNNOTCHED SPECIMENS OF ABS-C NORMALIZED STEEL SUBJECTED TO ZERO-TO-TENSION FATIGUE LOADING.

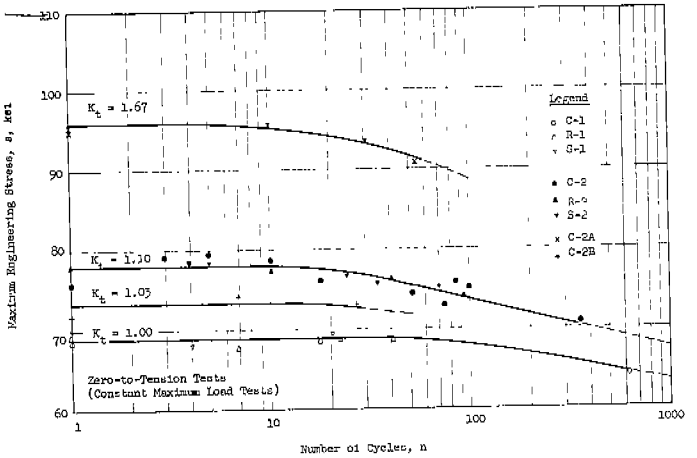

FIG. 25. S-N CURVES FOR ZERO-TO-TENSION LOW-CYCLE FATIGUE TESTS OF ABS-C NORMALIZED STEEL.

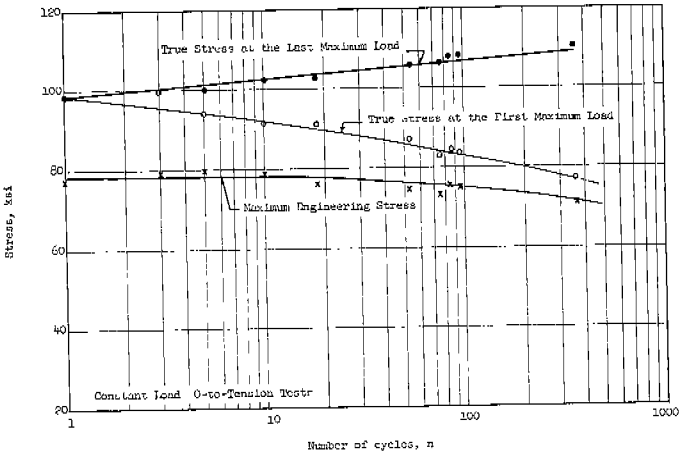

FIG. 26. TRUE AND NOMINAL STRESSES VS. LIFE FOR C-2 SPECIMENS OF ABS-C NORMALIZED STEEL.

a marked change or transition in true stress behavior can be expected at an intermediate life and might provide a means of differentiating between plastic low-cycle fatigue and long-life fatigue.

When plotted on the basis of engineering stress it is found that the low-cycle portion of the s-n curve is rather flat. This flatness is more pronounced for the plain specimens than for those which are notched and suggests that the maximum average stress is not a good discriminator of low-cycle life in zero-to-tension fatigue tests. As a result, many investigators present low-cycle fatigue data in terms of strain rather than stress. As shown in Figs. 27, 28 and 29 the strain (engineering strain for the series 1 specimens and true strain for the series 2 specimens) at the first maximum load is a more sensitive parameter than the maximum engineering stress for the presentation of fatigue data for failure in less than approximately 400 cycles. Straight lines can be used most effectively to represent the data.

Test data for sustained maximum load fatigue tests are listed in Table 4. Figure 30 shows the relationship between the initial true strain at the maximum load vs. the time at the maximum load for one-cycle sustained load tests. Thus, typical of a creep-rupture relationship, the time to failure was

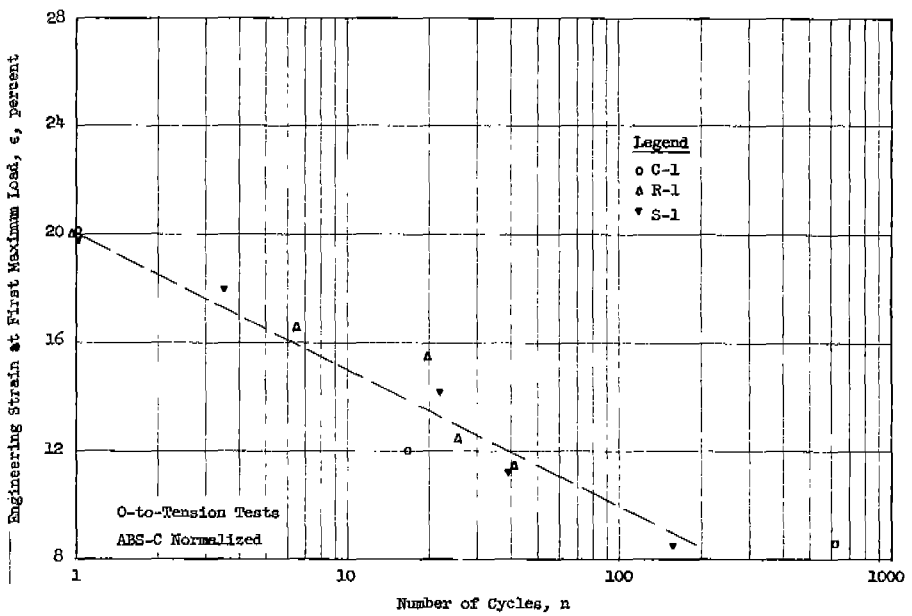

FIG. 27. ENGINEERING STRAIN AT FIRST MAXIMUM LOAD VS. LIFE FOR C-1, R-1 AND S-1 SPECIMENS.

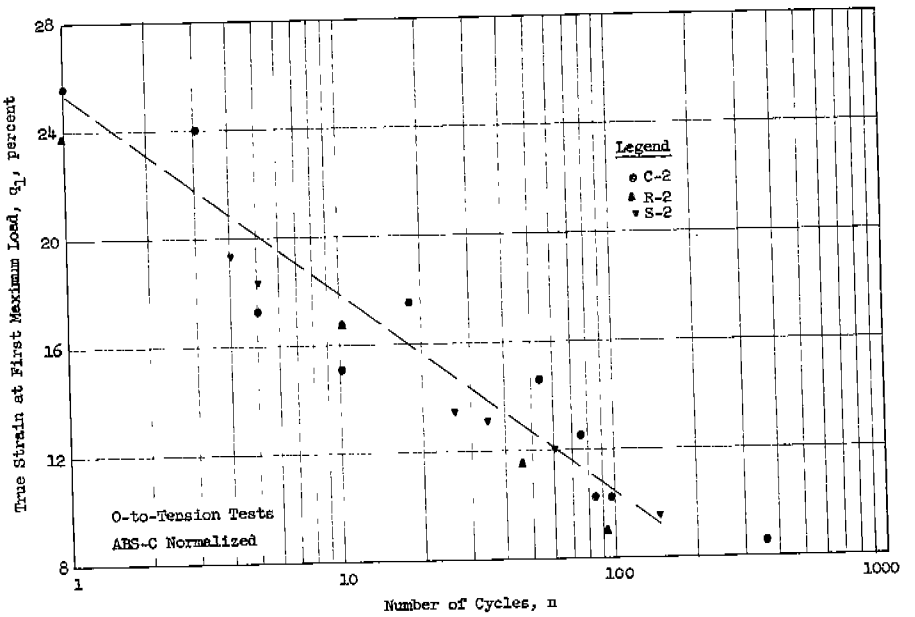

FIG. 28. TRUE STRAIN AT FIRST MAXIMUM LOAD VS. LIFE FOR C-2, R-2 AND S-2 SPECIMENS.

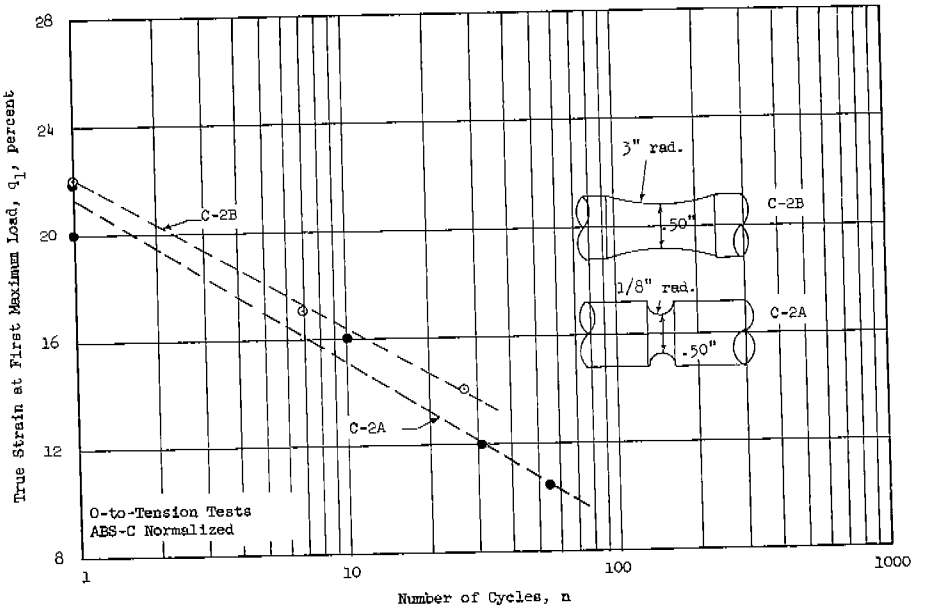

FIG. 29. TRUE STRAIN AT FIRST MAXIMUM LOAD VS. LIFE FOR C-2A, C-2B SPECIMENS.

found to increase logarithmically with a decrease in the initial strain. Other tests in this series were conducted under repeated loads. In Fig. 31 are shown the load-time curve for three of the type C-2A specimens (C-2A-CN 168, C-2A-CN 166, and C-2A-CN 169) that were subjected to approximately the same load, but with different lengths of time for the sustained maximum load. The lives of these specimens varied from 6 to 23 cycles as a result of varying the time at the cyclic maximum load from 10 minutes to 1 minute. The relationships

TABLE 4. ZERO-TO-TENSION SUSTAINED LOAD FATIGUE TEST DATA

Specimen No.	Maximum Stress ksi, s	Cycles to Failure, n	Strain at First Max. Load %	Time per Cycle at Max. Load, Minutes
C-2-CN109	74.8	1.0	17.2	21.0
C-2-CN111	75.1	1.0	19.0	7.5
C-2-CN112	77.0	2.2	17.0	5.0
C-2-CN113	76.5	1.0	17.5	16.0
C-2-CN116	77.4	3.0	18.0	2.5
C-2A-CN163	93.4	1.0	21.0	0.5
C-2A-CN164	91.4	1.0	13.6	44.0
C-2A-CN165	92.2	1.0	16.0	6.25
C-2A-CN166	90.1	11.0	11.6	5.0
C-2A-CN167	92.4	1.0	15.5	10.5
C-2A-CN168	90.4	6.3	11.6	10.0
C-2A-CN169	89.8	23.0	11.5	1.0

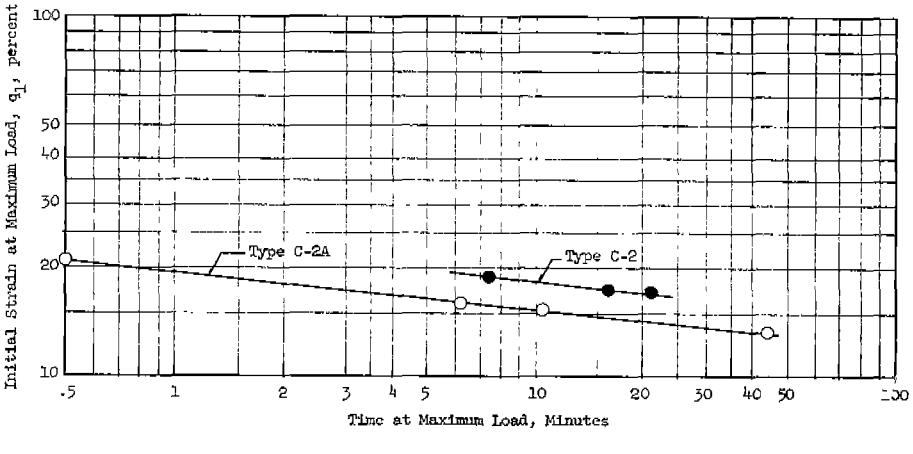

FIG. 30. STRAIN VS. TIME AT MAXIMUM LOAD IN ONE-CYCLE SUSTAINED LOAD TESTS FOR TYPE C-2, C-2A SPECIMENS OF ABS-C NORMALIZED STEEL.

between the time at the maximum load per cycle and the fatigue life for specimens with approximately the same initial true strains are shown in Fig. 32. It is evident that the load pattern or length of time sustained at the maximum load has a marked effect on the low-cycle fatigue life in the zero-to-tension tests at a constant maximum load.

It is generally found that the rate of cycling, if below approximately 3000 cpm, has no significant effect on the fatigue strength of a member under long-life fatigue. However, in the case of low-cycle fatigue it can be expected that the loading rate, the magnitude of the load, and the length of time that the maximum load is sustained will all affect the behavior. Lower rates of loading, higher loads and longer periods of sustained load will each tend to reduce the number of cycles to failure.

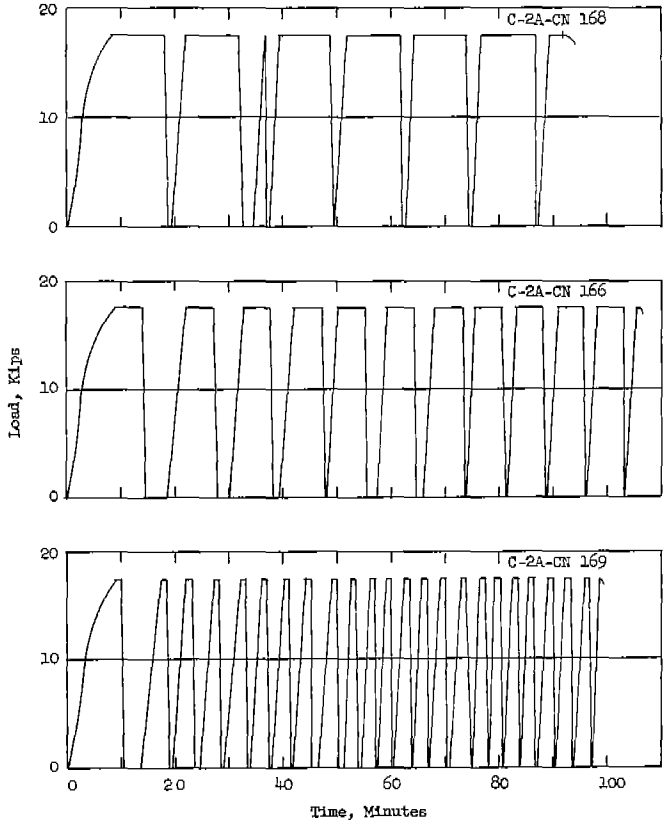

FIG. 31. LOAD-TIME PATTERN FOR SPECIMENS SUBJECTED TO INTERMITTENTLY SUSTAINED LOADINGS FOR TYPE C-2A SPECIMENS OF ABS-C NORMALIZED STEEL.

Reversed-Load Tests. The results of reversed-load fatigue tests for several types of specimens prepared and tested in various ways are listed in Table 5, and plotted in Figs. 33 and 34. In both figures, it may be seen that the direction of the first loading (whether tension or compression) appears to have a small effect on the fatigue behavior of types C-2 and C-2A specimens at lives less than 100 cycles. Figure 33 shows also the effect of the direction of polishing; specimens prepared with longitudinal polishing had a somewhat higher fatigue strength than those with transverse polishing. In the same figure, it may be seen that there is no aging effect in the life region between 10^3 and 10^4 cycles for specimens aged at lives ranging from 1 to 500 cycles and then tested to failure.

The low-cycle reversed load fatigue behavior of Types C-2A and C-2A1 specimens is shown in Fig. 34. The specimen with the higher stress concentration, type C-2A, had a higher strength at n = 1, but gradually lost this advantage. The fatigue resistance of the type C-2A specimens is found to be equal to that of the type C-2A1 specimens at a life of approximately 10^4 cycles, equal to that of the plain type C-2 specimens at a life of approximately 10^3 cycles and, at greater lives, the fatigue resistance of the type C-2A specimens would be lower than the others. This general behavior is similar to the behavior obtained in the zero-to-tension tests and similar to the behavior of notched specimens tested and reported by other investigators.

In the reversed-load tests the specimen diameter was measured after each loading and the corresponding true strains then computed. As a result, strain histories of the type shown in Figs. 35 and 36 were obtained. It is evident that in tests where load limits are maintained constant the plastic strain limits vary throughout the tests. In these particular tests, the plastic true strain limits increased continuously with an increase in the number of load applications and then exhibited a major jump to the ultimate plastic true strain in the final cycles.

TABLE 5. SUMMARY OF REVERSED-LOAD FATIGUE TEST DATA.

Specimen No.	Stress Cycle ksi	Number of Cycles N_c, Visible Crack	Number of Cycles N_f, Failure	$\frac{N_c}{N_f}$	
		(Transversely Polished)			
C-2-CN120	± 83 (C)*	-	1	-	
C-2-CN138	± 78 (T)*	-	2	-	
C-2-CN132	± 79 (C)	-	4	-	
C-2-CN135	± 74 (T)	-	6	-	
C-2-CN133	± 74 (C)	-	16	-	
C-2-CN124	± 69 (T)	-	34	-	
C-2-CN117	± 70 (C)	-	48	-	
C-2-CN505	± 75	-	35	-	
C-2-CN501	± 65	395	545	.72	
C-2-CN502	± 55	1295	2543	.51	
C-2-CN504	± 45	2716	4149	.65	
C-2-CN503	± 40	12200	17244	.71	
C-2A-CN304	± 100	-	1	-	
C-2A-CN302	± 92 (C)	13	16	-	
C-2A-CN310	± 87 (T)	-	23	-	
C-2A-CN306	± 87 (C)	23	29	.78	
		(Longitudinally Polished)			
C-2-CN410	± 75	118	224	0.53	
C-2-CN404	± 75	85	130	0.65	
C-2-CN403	± 70	240	400	0.60	
C-2-CN409	± 65	500	750	0.67	
C-2-CN402	± 60	1300	1900	0.68	
C-2-CN408	± 55	1800	2500	0.72	
C-2-CN401	± 50	2600	5200	0.50	
C-2-CN514	± 50	-	5306	-	
C-2-CN406	± 50	6600	7900	0.84	
C-2-CN405	± 45	10000	12600	0.79	
C-2-CN407	± 45	10200	12800	0.80	
C-2-CN509	± 60	-	1544	(aged after 1 cycle)	
C-2-CN506	± 55	-	3555	(aged after 1 cycle)	
C-2-CN511	± 50	-	7647	(aged after 1 cycle)	
C-2-CN513	± 50	-	7495	(aged after 204 cycles)	
C-2-CN515	± 50	-	6651	(aged after 509 cycles)	
C-2-CN512	± 45	-	13643	(aged after 1 cycle)	
C-21-CN411	± 50	2400	3400	.71	
C-21-CN415	± 41	12502	6292	.77	
C-2A-CN420	± 70	329	394	.84	
C-2A-CN419	± 60	610	1080	.56	
C-2A-CN416	± 50	2100	3000	.70	
C-2A-CN417	± 40	2900	5500	.53	
C-2A-CN418	± 33	10200	24300	.42	
C-2A1-CN423	± 60	-	240	-	
C-2A1-CN421	± 50	1000	1700	.59	
C-2A1-CN422	± 40	2700	4400	.61	
C-2A1-CN424	± 35	9842	18963	.52	
C-2A1-CN425	± 30	12700	28200	.45	

* (C) - First load applied in Compression.

(T) - First load applied in Tension.

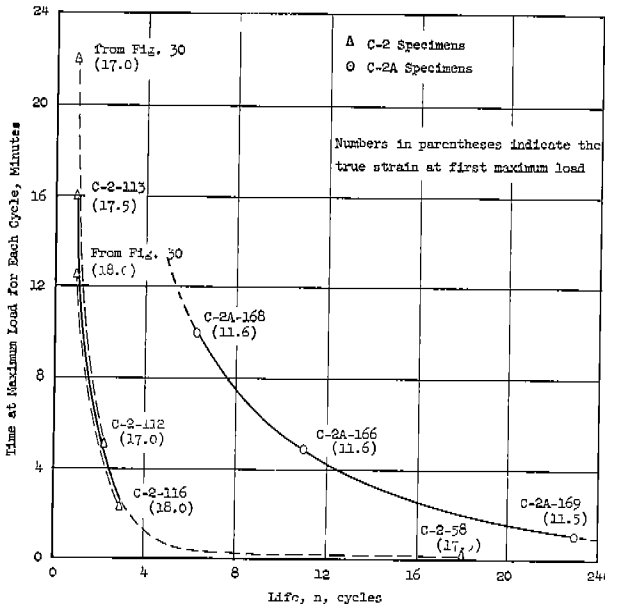

FIG. 32. TIME AT MAXIMUM LOAD VS. LIFE FOR SELECTED SERIES 2 SPECIMENS OF ABS-C NORMALIZED STEEL SUBJECTED TO ZERO-TO-TENSION FATIGUE LOADINGS.

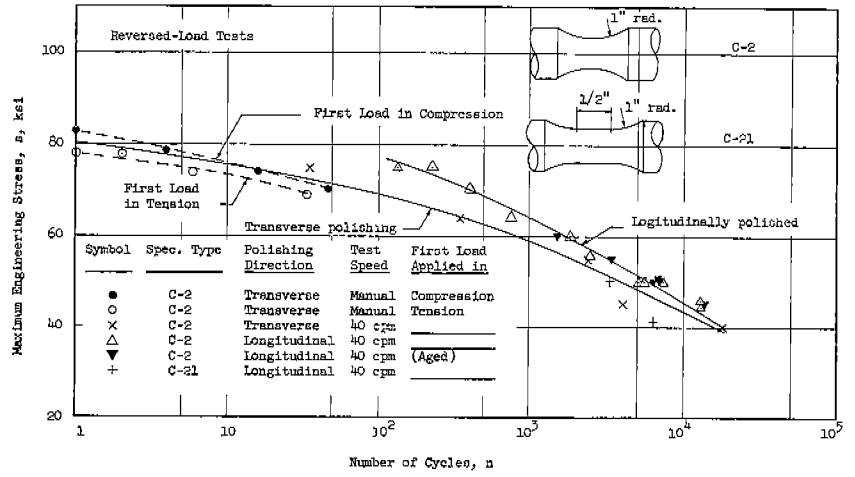

FIG. 33. S-N CURVES FOR TYPE C-2 AND C-21 SPECIMENS OF ABS-C NORMALIZED STEEL IN REVERSED-LOAD FATIGUE TESTS.

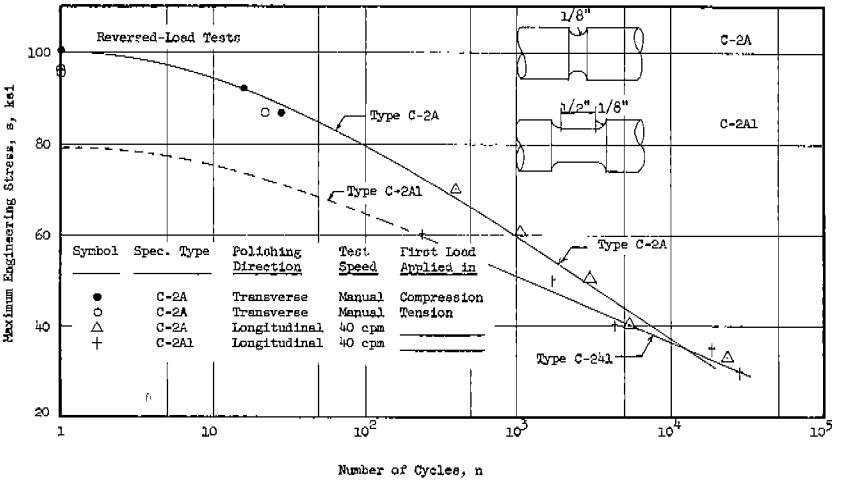

FIG. 34. S-N CURVES FOR TYPE C-2A AND C-2A1 SPECIMENS OF ABS-C NORMALIZED STEEL IN REVERSED-LOAD FATIGUE TESTS.

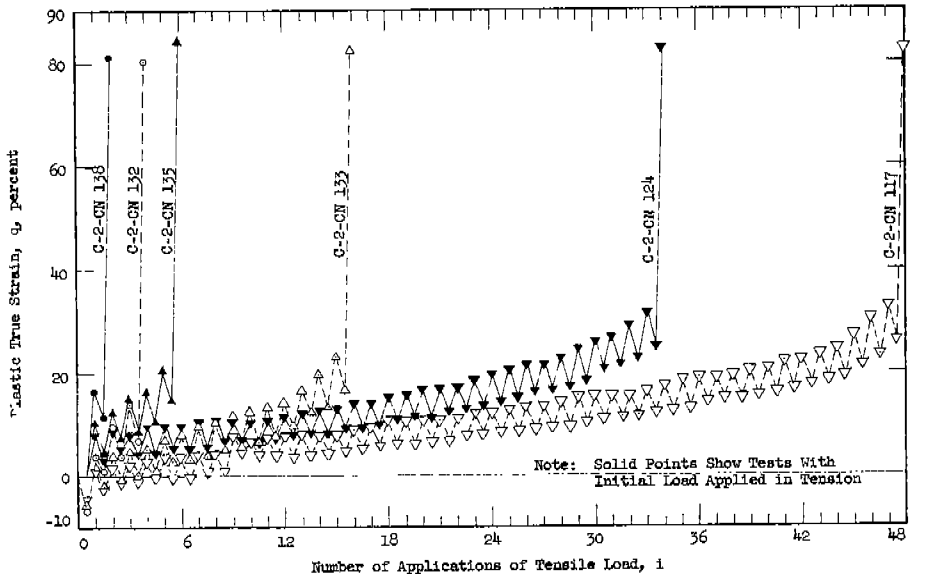

FIG. 35. STRAIN HISTORY FOR TYPE C-2 SPECIMENS OF ABS-C NORMALIZED STEEL IN REVERSED-LOAD LOW-CYCLE FATIGUE TESTS.

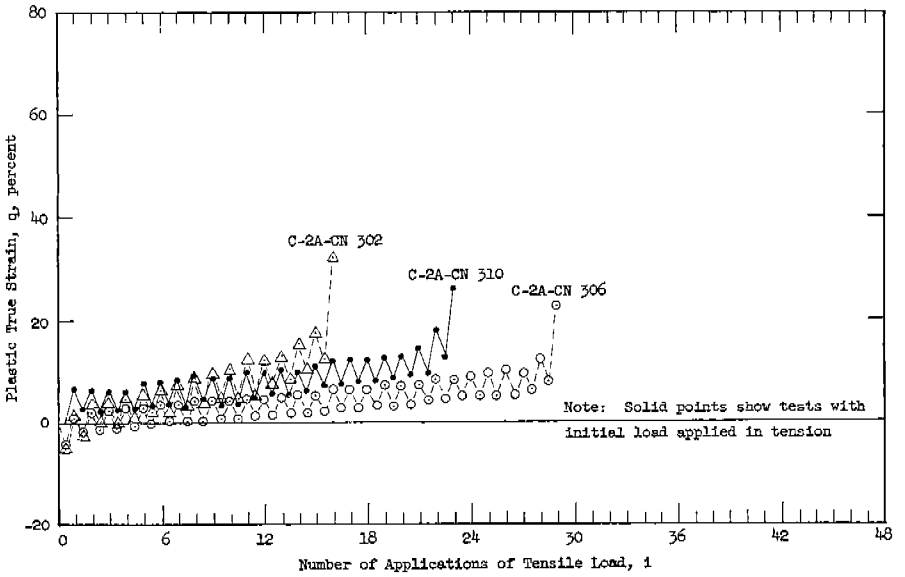

FIG. 36. STRAIN HISTORY FOR TYPE C-2A SPECIMENS OF ABS-C NORMALIZED STEEL IN REVERSED-LOAD LOW-CYCLE FATIGUE TESTS.

The specimens tested at 40 cpm and high stresses heated up during the tests. Thermocouples were attached to a number of selected specimens to determine the magnitude of the heat increase with respect to the number of

cycles. In general it was found that the temperature of the specimens increased rapidly initially and then gradually came to a steady-state value as shown in Fig. 37. Here it may be seen that the rate of initial temperature change and the level of the steady-state temperature both increased with an increase in the magnitude of the applied stresses.

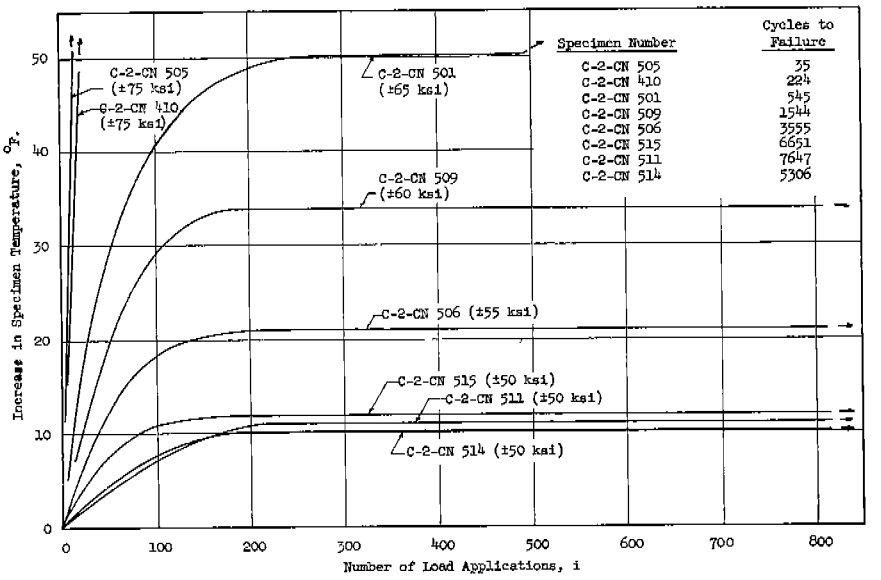

FIG. 37. SURFACE TEMPERATURE VARIATIONS OF SELECTED TYPE C-2 SPECIMENS OF ABS-C NORMALIZED STEEL DURING REVERSED LOAD LOW-CYCLE TESTS.

In the reversed-load tests the appearance of visible cracks was noted and has been related to the number of cycles to failure. This relationship, as presented in Fig. 38, may be represented approximately by the equation,

$$N_c = N_f^{0.95} \qquad (9)$$

A relatively small scatter band was obtained in these tests and would probably have been considerably smaller if more refined methods had been used to determine the time of crack initiation.

A variety of fractures and lives have been obtained in the reversed-load tests, depending upon the magnitude of the applied load. A number of

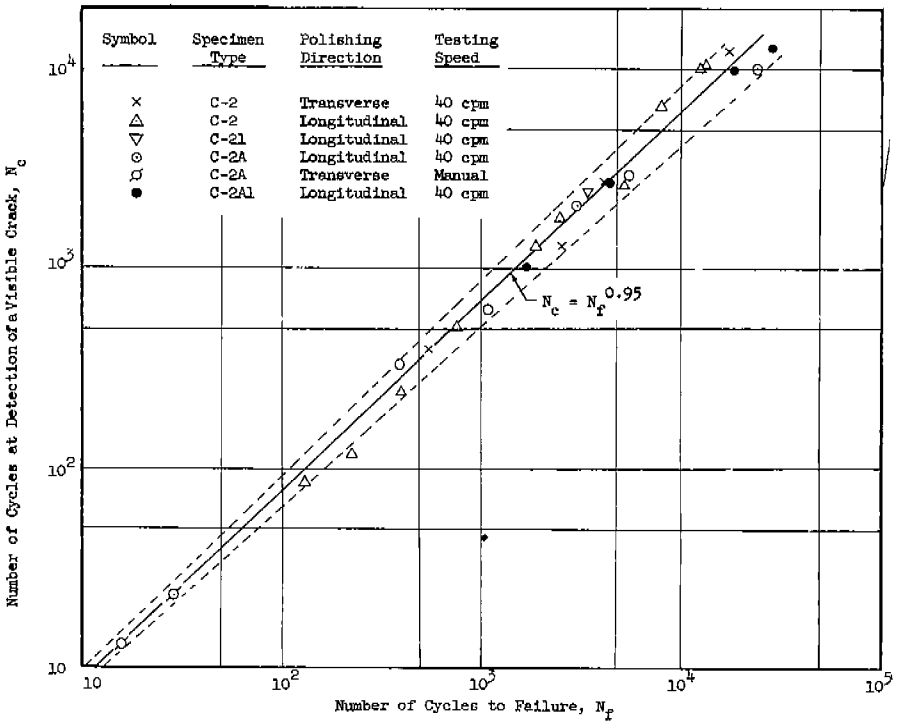

FIG. 38. NUMBER OF CYCLES AT DETECTION OF A VISIBLE CRACK VS. NUMBER OF CYCLES TO FAILURE FOR ABS-C NORMALIZED STEEL SPECIMENS.

typical fractures may be seen in Fig. 39. In this figure are shown four type C-2, one type C-2A and one type C-2Al specimens. The four type C-2 specimens demonstrate the effect of stress magnitude and indicate that there are more cracks in the specimens tested at the higher stresses than those tested at low stresses. In the three specimens of Fig. 39(b) the effect of specimen geometry is portrayed. The larger radius provides a more irregular fracture and a marked increase in life.

9. Cyclic Deformation Tests

A total of thirty-five type C-2 specimens were tested at constant relative-strain ratios of -1/4, -1/2, -3/4 and -1. Schematic q - n (strain vs. cycles) diagrams illustrating the cyclic strains for each of these r-ratios are shown in Fig. 13. The results of these tests are listed in Table 6 and

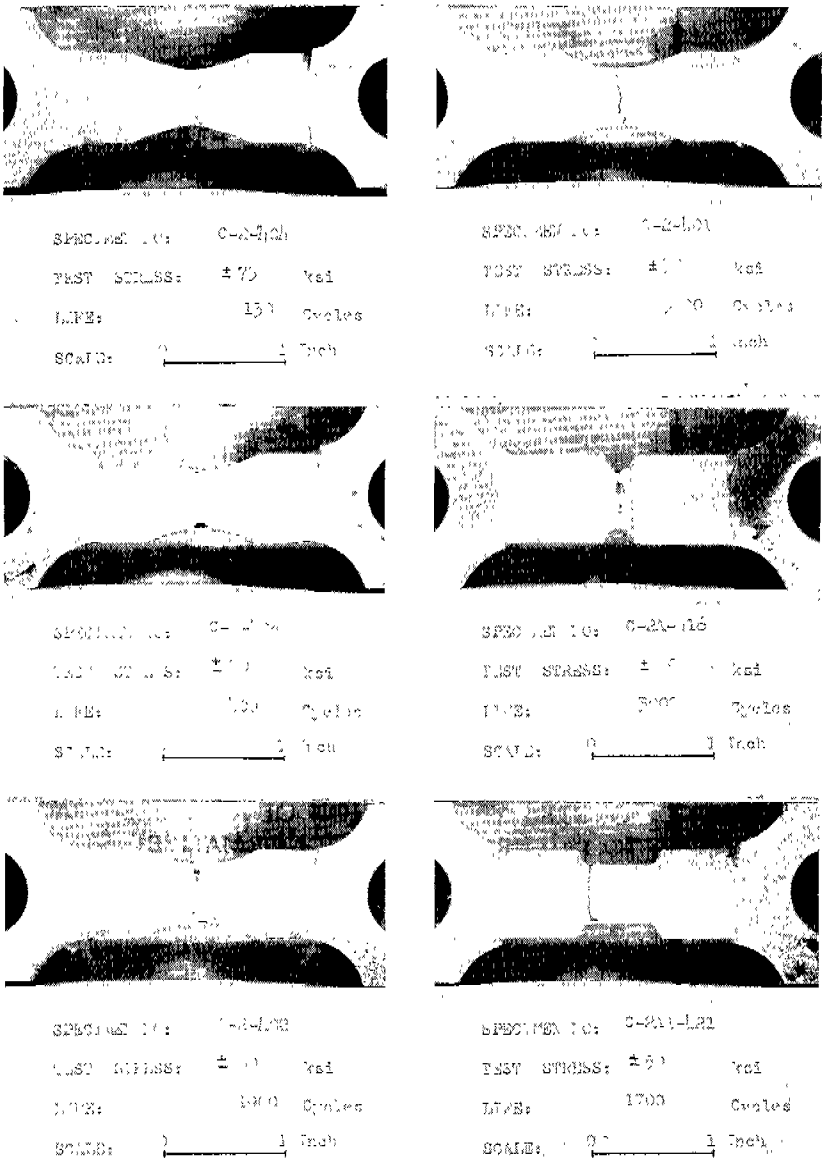

(a) Effect of Stress Level (b) Effect of Specimen Type

FIG. 39. TYPICAL FRACTURES FROM REVERSED-LOAD LOW-CYCLE FATIGUE TESTS.

plotted in Figs. 40, 41 and 42 for the three steels tested. It may be seen that straight lines with slopes that vary with the r-ratios fit the data quite well. These data may be further combined by dividing all plastic true strain values by their corresponding values of Δq_{tl}, the plastic true strain

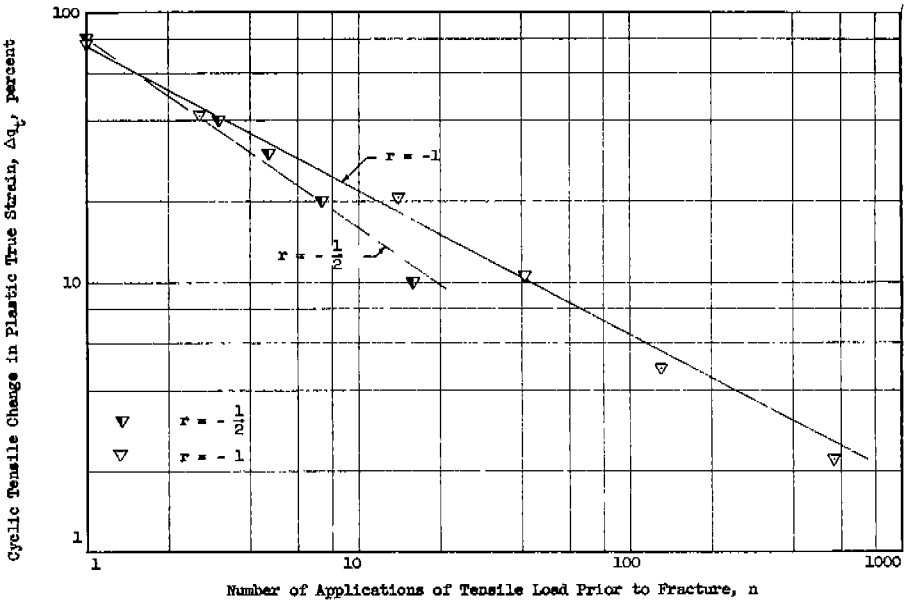

FIG. 40. CYCLIC DEFORMATION TEST RESULTS FOR TYPE C-2 SPECIMENS OF ABS-C NORMALIZED STEEL.

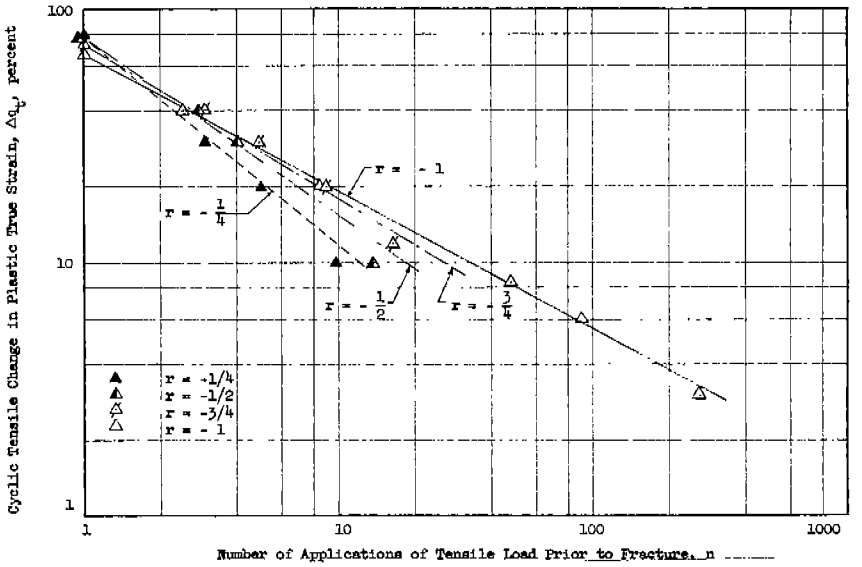

FIG. 41. CYCLIC DEFORMATION TEST RESULTS FOR TYPE C-2 SPECIMENS OF ABS-C AS-ROLLED STEEL.

for one-cycle. These strain values are said to be "normalized."[4] Figure 43 is a diagram with normalized cyclic tensile change in plastic true strain plotted against n, the cycles to failure, on a log-log basis for all three steels tested. When the test data are presented in this manner, there does not seem to be any effect of material on the slope of these relationships.

TABLE 6. RESULTS OF CYCLIC DEFORMATION TESTS.

Relative-Strain Ratio $r = \frac{\Delta q_c}{\Delta q_t}$	Specimen No.	Cyclic Tensile Change in Plastic True Strain percent Δq_t	Normalized Cyclic Tensile Change in Plastic True Strain, percent $\Delta q_t / \Delta q_{t1}$	Cycles to Failure n
-1/4	C-2-CA*	80	100	1
	C-2-CA108	30	38	3
	C-2-CA16	20	25	5
	C-2-CA7	10	13	10
-1/2	C-2-CN*	83	100	1
	C-2-CN518	40	49	3
	C-2-CN517	30	36	5
	C-2-CN516	20	24	7
	C-2-CN519	10	12	16
-1/2	C-2-CA*	77	100	1
	C-2-CA112	40	52	3
	C-2-CA104	30	39	4
	C-2-CA12	20	26	6
	C-2-CA8	10	13	14
-1/2	C-2-E*	75	100	1
	C-2-E111	40	53	3
	C-2-E108	30	40	4
	C-2-E107	20	27	7
	C-2-E112	10	13	14
-3/4	C-2-CA*	72	100	1
	C-2-CA113	40	56	3
	C-2-CA103	30	42	5
	C-2-CA13	20	28	9
	C-2-CA3	12	17	17
-1	C-2-CN*	76	100	1
	C-2-CN508	42	55	3
	C-2-CN507	21	27	14
	C-2-CN524	11	14	41
	C-2-CN522	5	6	130
	C-2-CN521	2	3	565
-1	C-2-CA*	66	100	1
	C-2-CA115	39	59	2
	C-2-CA5	20	30	9
	C-2-CA14	8	13	48
	C-2-CA4	6	9	90
	C-2-CA116	3	5	261
-1	C-2-E*	66	100	1
	C-2-E106	40	61	2
	C-2-E105	19	29	10
	C-2-E15	8	13	42
	C-2-E6	6	9	91
	C-2-E7	4	7	182
	C-2-E13	3	4	322

* Interpolation for "one-cycle" test results.

Evans[5] obtained a constant true strain at fracture in his repeated tension tests, regardless of the number of cycles applied prior to fracture. In the program reported herein it was observed that for a group of C-2 type

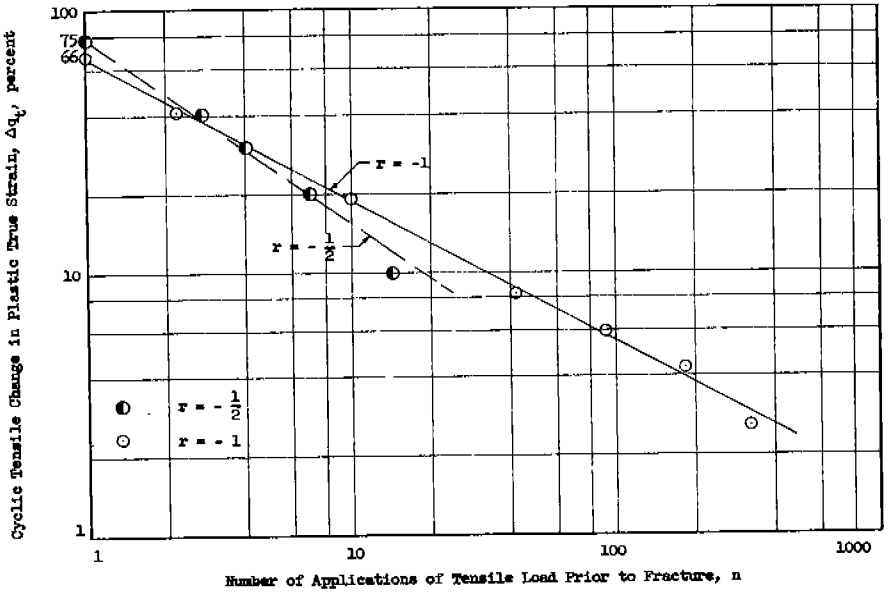

FIG. 42. CYCLIC DEFORMATION TEST RESULTS FOR TYPE C-2 SPECIMENS OF RIMMED STEEL.

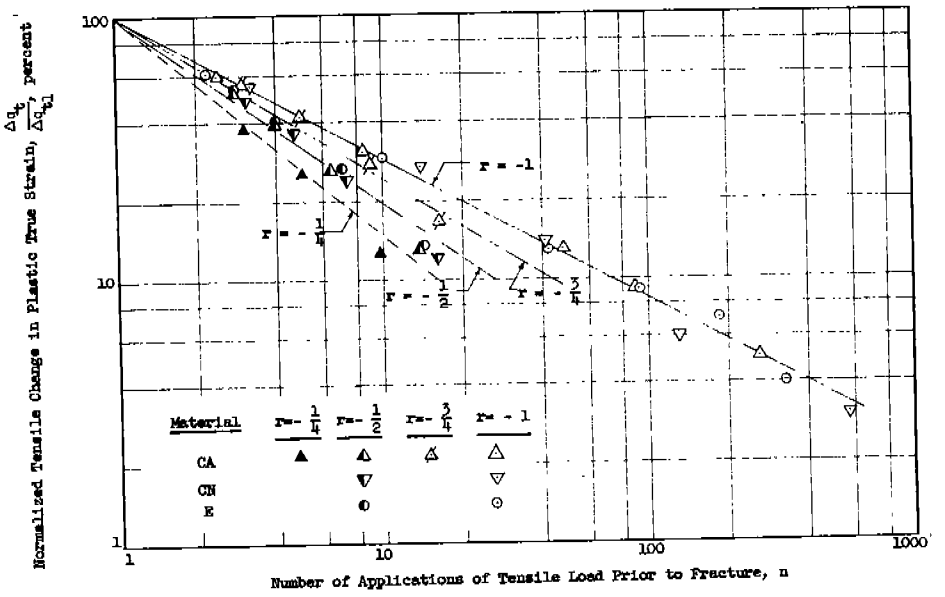

FIG. 43. CYCLIC DEFORMATION TEST RESULTS FOR TYPE C-2 SPECIMENS OF ALL TEST MATERIALS PLOTTED IN NORMALIZED FORM.

TABLE 7. PLASTIC TRUE STRAIN AT FRACTURE OF SPECIMENS IN ZERO-TO-TENSION CYCLIC LOAD TESTS

Specimen No.	Max. Stress, ksi	Cycles to Failure n	Plastic True Strain at Fracture, percent q_f
C-2-CN109	75	1	82
C-2-CN111	75	1	82
C-2-CN113	77	1	82
C-2-CN115	75	1	80
C-2-CN112	77	3	80
C-2-CN107	79	3	81
C-2-CN116	77	4	80
C-2-CN103	79	5	79
C-2-CN104	79	10	79
C-2-CN58	76	18	77
C-2-CN59	75	53	83
C-2-CN33	73	75	84
C-2-CN106	76	84	81
C-2-CN105	75	96	81
C-2-CN108	71	352	84

CN-steel specimens subjected to various amounts of repeated tension, regardless of the number of cycles of tensile load before fracture, the final value of plastic true strain at fracture was more or less constant for the zero-to-tension low-cycle tests. The plastic strain data from these tests are listed in Table 8 and also plotted in Fig. 44. It is evident that, in these tests, regardless of the number of cycles of tensile load applied before fracture, the final value of plastic true strain at fracture is more or less a constant for the materials studied and at least for lives as great as 350 cycles. Therefore, it is reasonable to conclude that for low-cycle fatigue tests in repeated tension only, i.e., $r = 0$, the cyclic tensile change in plastic true strain is linearly accumulative.

In the cyclic deformation tests where the limits in true strain were monitored in each cycle, the magnitude of load necessary to cause these strain changes varied, generally increased, from cycle to cycle. In Figs. 45 and 46 are shown the envelope of true stress histories of cyclic deformation of type C-2 specimens of the CN steel tested at relative-stress ratios of -1/4

and -1. In general, there was an increase also in true stress with increasing number of cycles. In such cases the specimen is said to have "strain-hardened" due to repeated loadings. It is also noted that generally there is more

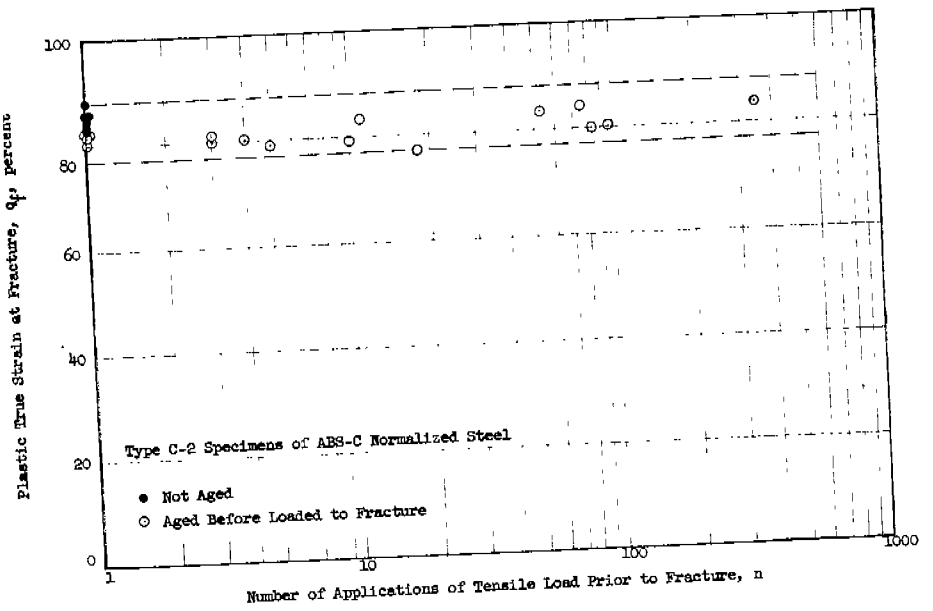

FIG. 44. PLASTIC TRUE STRAIN AT FRACTURE OF SPECIMENS SUBJECTED TO REPEATED TENSILE LOADS.

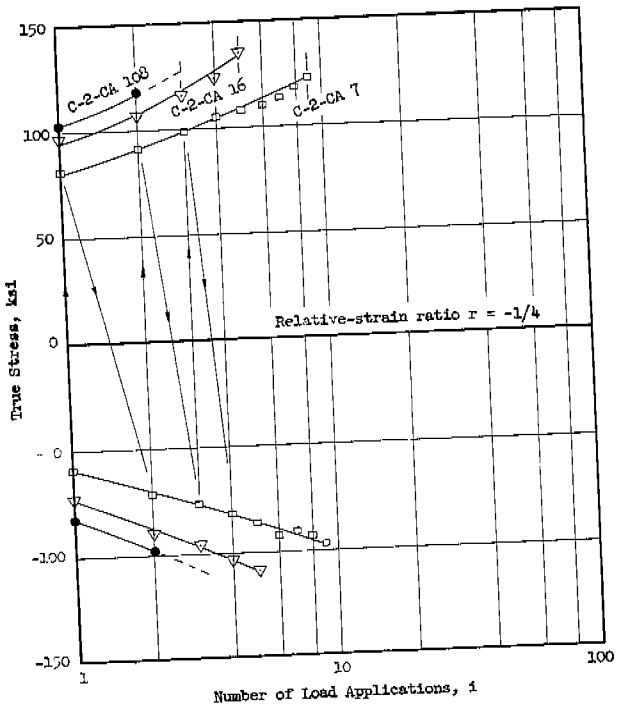

FIG. 45. TYPICAL RELATIONSHIPS BETWEEN TRUE STRESS AND NUMBER OF LOAD APPLICATIONS FOR RELATIVE-STRAIN RATIO OF - 1/4.

strain hardening in specimens subjected to higher strain values and lower relative-strain ratios. The true stress curves of Fig. 45 at a relative-strain ratio of -1/4 are much steeper and show a greater change with life than do those of Fig. 46 and thereby show a greater "strain-hardening" effect

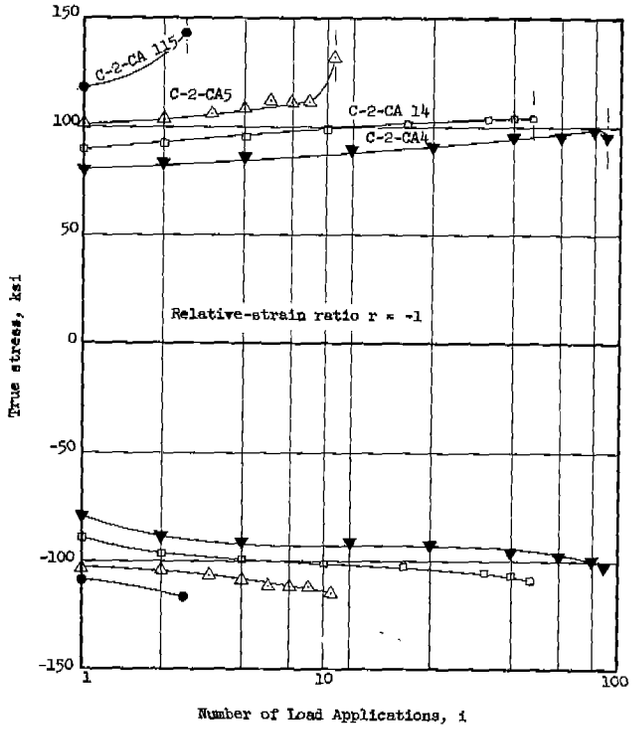

FIG. 46. TYPICAL RELATIONSHIPS BETWEEN TRUE STRESS AND NUMBER OF LOAD APPLICATIONS OF RELATIVE-STRAIN RATIO OF -1.

Apparently under a complete reversal of strain, such as that shown in Fig. 46, the compressive straining tends to "strain soften" or reduce the "strain hardening" of the material.

Some of the fractured specimens are shown in Fig. 47. In the top row, three "one-cycle" test specimens are presented, one for each material. It may be noted that vertical cracks are present on the surface of the E-steel specimen shown on the right side of the page. These vertical cracks often resulted when large compression loads were employed, but only for E-steel specimens. In the second row three CA-steel specimens are shown after being tested at

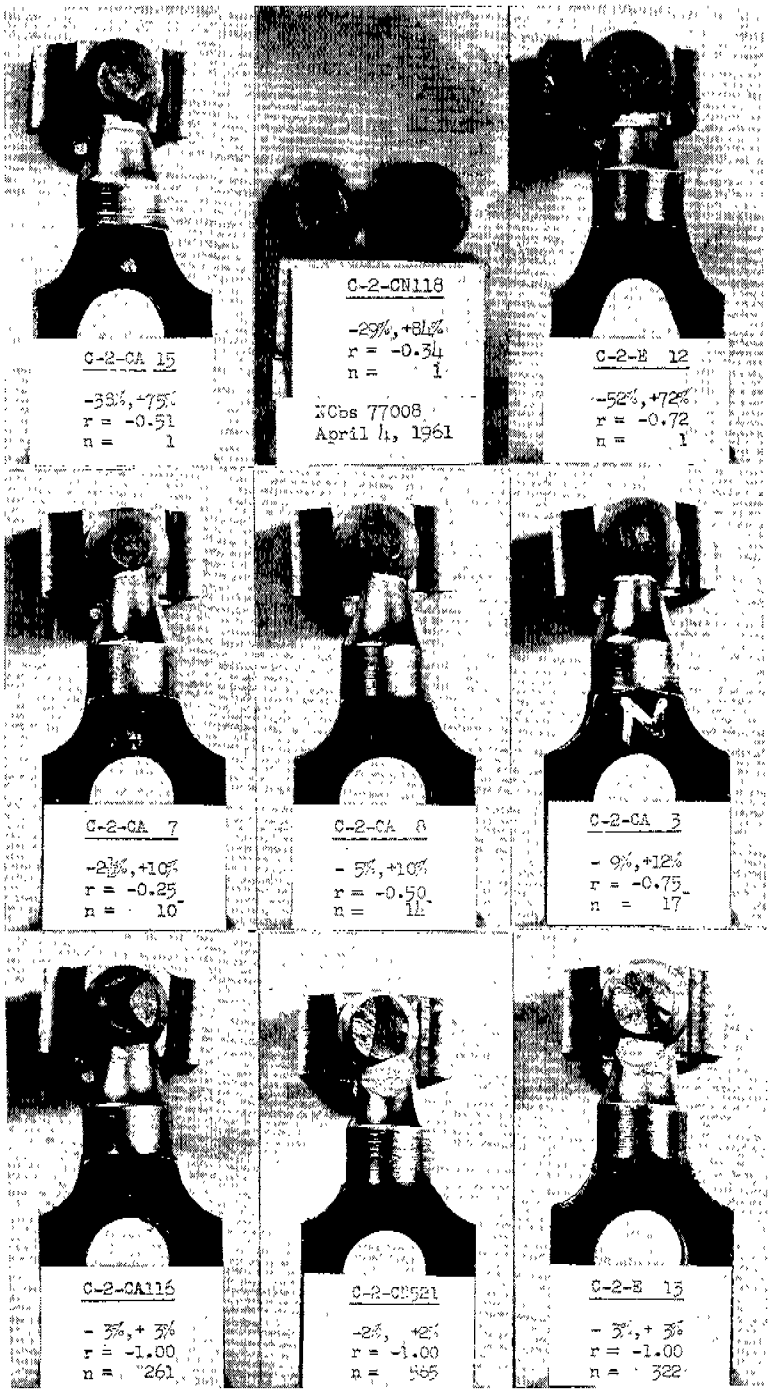

FIG. 47. VARIOUS FRACTURES RESULTED FROM CYCLIC DEFORMATION TESTS.

relative-strain ratios of -0.25, -0.50, and -0.75. These gave lives of 10, 14, and 17 cycles respectively. All six specimens exhibited cup-and-cone type

of fractures. In the bottom row of Fig. 47 are shown specimens of the three steels tested with r = -1. There was evidence of numerous surface cracks on the specimens thereby demonstrating that these specimens were close to failure at a number of locations.

IV. A LOW-CYCLE FATIGUE HYPOTHESIS

10. Other Investigations of Cyclic Deformation Low-Cycle Fatigue Tests

A. Experimental Results

In 1912, Kommers[6] concluded from a series of cyclic bending tests that the magnitude of the cyclic deflection was an important factor in low-cycle fatigue studies. Later, "unit-deformations" or "engineering strains" were used as test parameters by various investigators to include the effect of possible variations in the initial gage length of the specimens. In recent low-cycle fatigue investigations there has been an increase in the use of "true strains." Nevertheless, the computations of "unit deformations," "engineering strains," and "true strains" are still based on the measurement of gross deformations or deflections of the specimens. It is to be noted that the distribution of "engineering strains" within a certain volume, or the distribution of "true strains" over a certain cross section is not always uniform, especially when appreciable changes in geometry, such as the occurrence of cracks, take place in the test section. Therefore, in the following discussions the word "strain" refers to a representation of some gross deformation or deflection experienced by a portion of the specimen rather than a very localized phenomenon as the word "strain" sometimes implies.

Evans[5] repeatedly applied tensile forces to produce constant increments of longitudinal plastic strain to axially-loaded specimens made of various metals. He observed that while the total engineering strain at fracture increased as a result of repeated loadings, the true strain at fracture remained constant in most cases. In Fig. 48, cyclic tensile changes in plastic engi-

neering strain, $\Delta\epsilon_t$, in percent vs. number of cycles to fracture N, are plotted on a log-log basis for a mild steel and a copper wire. It may be seen that,

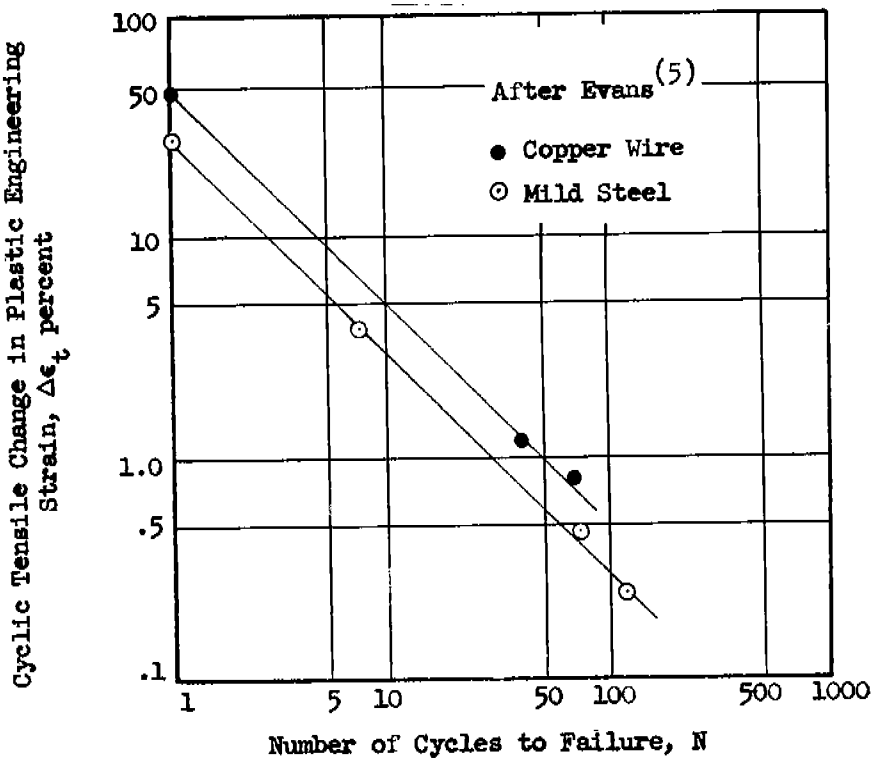

FIG. 48. TYPICAL LOG $\Delta\epsilon_t$ VS. LOG N DIAGRAMS OBTAINED FROM REPEATED TENSION TESTS.

for specimen lives less than about 100 cycles, straight lines with a slope of -1 fit the test points quite well.

Low[7,8] carried out bending fatigue tests on two aluminum alloys and three steels at room temperature, and Johansson[9] conducted cyclic bending tests on three steels at various temperatures ranging from +20° to +500°C. Again, both investigators found a linear relationship between cyclic strains and corresponding specimen lives on log-log plots.

Coffin and his associates[10,11,12,13] have conducted extensive low-cycle fatigue tests on 347 stainless steel specimens with thermal and mechanical strain-cycling. In their earlier works, engineering strains were used as a basis for their tests. Recently, they have placed emphasis on the usage of

true strains both in the testing and in the analysis of their test results. In analyzing their own data as well as reversed strain test data of others, it was found that straight lines with a slope of approximately -0.50 best fit the test points on log Δq_t (cyclic tensile change in plastic true strain) vs. log N (number of cycles to failure) diagrams as shown in Fig. 49. However, Douglas and Swindeman[14] tested Hastelloy B, beryllium, and Inconel at temperatures above +1300°F and obtained for these materials straight lines with slopes ranging from -0.58 to -0.81 on a log $\Delta\epsilon_t$ vs. log N diagram. In 1959, Majors,[15] in reversed-strain tests on axially-loaded specimens of titanium and nickel at high temperatures, found the slope to vary from -0.48 to -0.51. More recently, Dubuc[16] found a slope of -0.53 for a low carbon steel and a brass in cyclic axial strain tests. These differences indicate that the slope of log $\Delta\epsilon_t$ (or log Δq_t) vs. log N lines may be a variable and depend upon the test conditions.

Many constant-deformation tests have been conducted on 2024 ST aluminum alloy. In 1949, Liu et al[19] carried out under axial-loading,

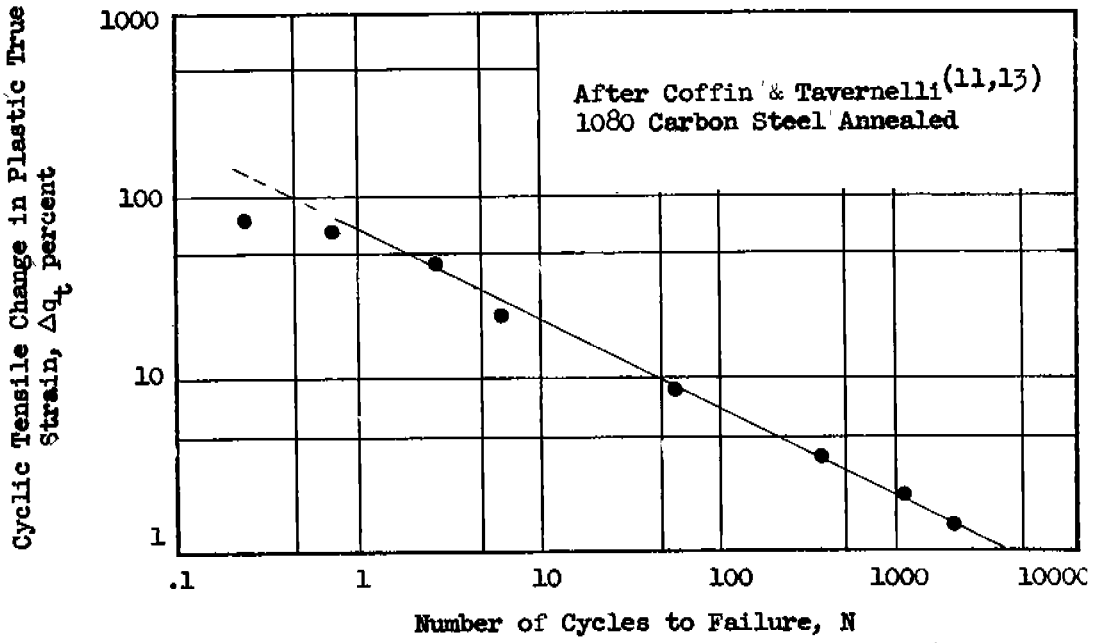

FIG. 49. TYPICAL LOG Δq_t VS. LOG N DIAGRAMS OBTAINED FROM REVERSED-STRAIN LOW-CYCLE FATIGUE TESTS.

reversed "true-strain" tests on this same alloy and to a maximum life of seven cycles. Following the exploratory experimental study made by Lin and Kirsch,[2] Pian and D'Amato[18] performed low-cycle fatigue tests on the same material but with variations in the absolute-strain ratio, R (i.e., ratio of cyclic minimum strain to cyclic maximum strain), and obtained data for lives up to 200 cycles. Later, D'Amato[4] carried the same type of test up to 10,000 cycles. These results also show that straight line relationships exist between the cyclic tensile change in plastic strain and the specimen life on a log-log scale. However, the slope of the lines was dependent upon the value of mean strains used.

Sachs et al[19,20] conducted both axial and bending low-cycle fatigue tests on specimens of A302 steel, 5454-0 aluminum, and 2024-T4 aluminum alloy. They report that the effect of mean strain becomes insignificant when the specimen lives are greater than 10,000 cycles.

In 1960, Mehringer and Felgar[21] reported a series of thermal strain-cycling tests on two high temperature alloys. Because of the low ductility possessed by both metals, the plastic strain values were too small to be measured with the desired accuracy and the test data had to be presented in terms of stress vs. life. This experience indicates one of the limitations on the use of cyclic plastic strain as a parameter in the case of low-ductility materials.

B. Analysis

Since Orowan[22,23] published his theory on the fatigue of metals in 1939, the results of many experimental studies have confirmed his prediction that a linear relationship exists between log $\Delta\epsilon_t$ and log N. In his original theory[22] emphasis was placed on the assumption that the distribution of stress in the material is not homogeneous. With an additional assumption that reversed local plastic deformations could cause a progressive work-hardening in the material, it was postulated that failure would occur at

points where either the stress or the total absolute plastic strain reached a critical stress or strain value. Later, Orowan[23] suggested the following expression for cyclic strain tests,

$$N \cdot \Delta\varepsilon_t = C \qquad (10)$$

where $\Delta\varepsilon_t$ is the cyclic tensile change in plastic engineering strain and C is a constant.

It is noted that Orowan's theory was originally intended to explain the fatigue behavior of an idealized material at points where stress-concentrations exist. Therefore, Eq. (10) must be modified for cases where strains representing the gross deformation of a specimen are used instead of the localized strain values. Nevertheless, this relationship has served as a basis for most of the hypotheses that have since been developed. Gross and Stout,[24] as well as Manson,[25] on the basis of reversed-strain tests, introduced a new variable, m, into Eq. (10)

$$N^m \cdot \Delta\varepsilon_t = C \qquad (11)$$

where m is an empirical constant obtained from the slope of the log $\Delta\varepsilon_t$ vs. log N diagram. Later, Coffin and his associates[11,13] found that a constant slope of -1/2, (i.e., m = 1/2) best fit their test data, as well as that of many others, and suggested the following expression:

$$N^{1/2} \cdot \Delta\varepsilon_t = \frac{q_f}{2} \qquad (12)$$

where q_f is the plastic true strain at fracture in tension.

Recently Martin[26] obtained the following expression on the basis of an energy criterion.

$$N^{1/2} \cdot \Delta\epsilon_t = \frac{q_f}{\sqrt{2}} \qquad (13)$$

Extensive comparisons made by Martin show that, for axial strain tests, the right hand term in Eq. (13) gives a better prediction of the constant C than that used in Eq. (12). However, the right hand term in Eq. (12) seems to give a better prediction of the constant C in the case of flexural strain tests conducted at high temperatures.

Gerberich[27,28] obtained Eq. (14) by taking into consideration the effect of mean strain on low-cycle fatigue lives.

$$N = \left(\frac{\epsilon_f' - \epsilon_o}{\epsilon}\right)^2 \qquad (14)$$

or

$$\epsilon \cdot N^{1/2} = \epsilon_f' - \epsilon_o \qquad (15)$$

where ϵ_f' is the apparent fracture ductility and ϵ_o is the mean strain. In later reports on the same program, Sachs et al[19,20] subsituted ϵ_{TR}, the total strain range, for ϵ, the plastic strain range. Test results on 2024-T4 aluminum alloy specimens[27,28] show that Eq. (14) describes very well the low-cycle fatigue behavior for various mean strains. However, it may be noted that (a) the apparent fracture ductility, ϵ_f' is a nominal value which is difficult to obtain; and (b) this relationship applies only to tests with positive mean strains, modifications must be made for other values of mean strain.

C. "One-Cycle" Tests

In the above-mentioned references, it is noted that most cyclic strain tests had been conducted under reversed-loadings. At the lowest

possible number of cycles in a reversed-strain test, the cyclic strain test simply becomes a tension test of specimens that have been plastically pre-compressed, or briefly a "one-cycle" test.

Bridgman[29] reported a series of "one-cycle" tests in which a low carbon steel was austempered* or tempered* to nine different conditions. Cylinders with an initial dimension of 1.5 in. both in diameter and in length were pre-compressed in three stages to a single value of true strain of -125 percent. At each stage, the compressive load was applied until the cylinder length was reduced to 2/3 of the original length, and then the cylinder was re-machined to its original 1 to 1 ratio of length to diameter. This process was repeated until the length of the cylinder was reduced to 0.42 in. (equivalent to a true strain of -125 percent). The cylinder was then cut to make three small tensile specimens (with the axes of two specimens along and one specimen transverse to the longitudinal axis of the cylinder). Then, tension tests were carried out in a specially designed test apparatus. The instantaneous diameter of the specimen was optically measured with a microscope attached to the apparatus. Test results are shown in Fig. 50, where the tensile change in plastic true strain at fracture, Δq_{tl}, is plotted against the amount of plastic true precompressive strain, q_{cl}, to which the members had been subjected (a single value of -125 percent in this case). Although only two points are shown for each of the nine heat treated conditions, it may be observed from these results that (a) the tensile strain at fracture is affected by the plastic true pre-compressive strain in the material and (b) the effect of pre-strain appears to vary with the heat treatment to which the material was subjected.

---

* Austempering involves the formation of bainite, the presence of which enables the material to possess relatively high impact resistance. Tempering produces tempered martensite in the material structure, and thus increases the ductility of the steel.

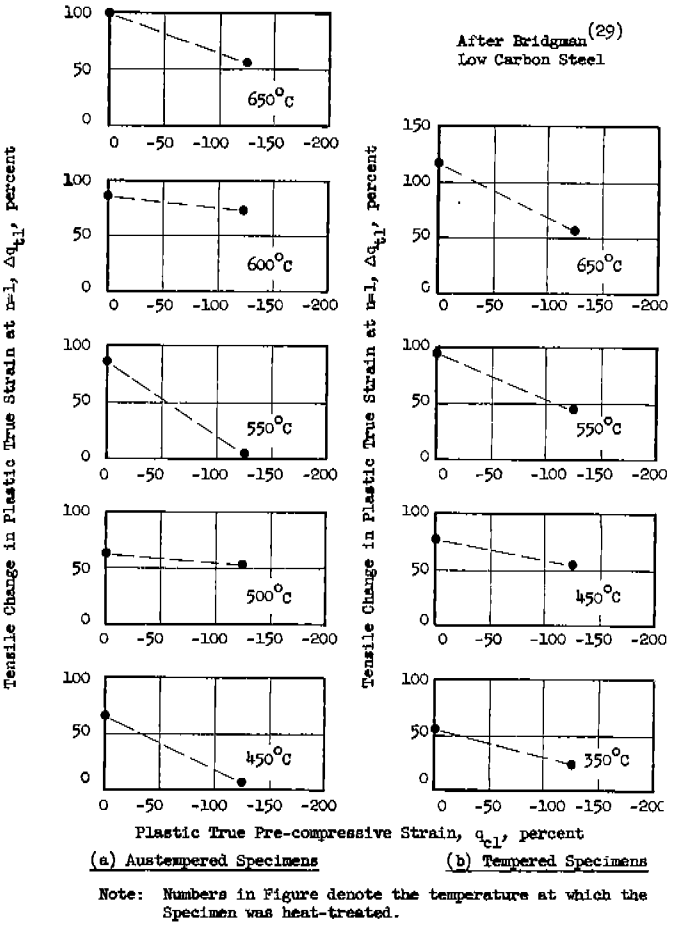

FIG. 50. BRIDGMAN'S "ONE-CYCLE" TEST DATA

Later in a study associated with an investigation of the initiation of brittle fracture, Drucker, Mylonas, and Lianis[30] conducted "one-cycle" tests on a rimmed ship steel often referred to as "E-steel" in a manner similar to that used by Bridgman except that more steps were taken in applying the compressive deformation and that standard tensile specimens were used. In addition, some specimens were artificially aged before the tension tests. The original information on the amount of pre-compressive strain was presented in terms of longitudinal strain ($\frac{\ell}{\ell_o} - 1$, where ℓ and ℓ_o are respectively the final and initial lengths of the cylinder used in pre-compression). By assuming that there is no volume change in the pre-compression operation, these longitudinal strains may be converted into equivalent true strains ($\ln \frac{\ell}{\ell_o}$). The

test results so converted are plotted in Fig. 51 where q_{tl} is the true strain at fracture and is equal to the algebraic sum of corresponding values of Δq_{tl}, the tensile change in plastic true strain, and q_{cl}, the plastic true pre-compression strain. It may be seen in Fig. 51 that, (a) the true strain at fracture decreases as the amount of pre-compressive strain increases, and (b) there is no significant difference in the strain at fracture between the artifically aged and unaged specimens. Furthermore, except for the data at the highest values of pre-compression, q_{cl}, approximately -63 percent, the data are in good agreement with that presented in Fig. 21 for the study reported herein and in spite of the differences in types of specimens and in the test procedures.

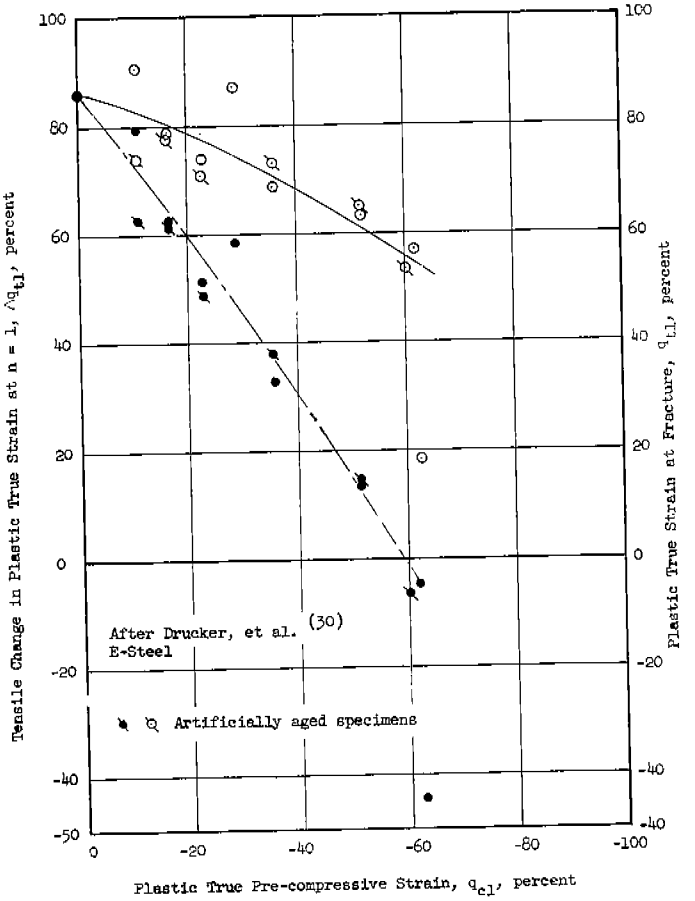

FIG. 51. BROWN UNIVERSITY "ONE-CYCLE" TEST DATA(30)

11. General Low Cycle Fatigue Hypothesis

A. Assumptions

Zener[31] has stated that "Fracture cannot occur independently of deformation." Although deformations can occur without necessarily causing fracture in the material, it is reasonable to assume that plastic deformation is cumulative in some manner toward the total fracture of the material.

Let us now examine more closely the empirical relationship shown in Eq. (11),

$$N^m \cdot \Delta\epsilon_t = C \tag{11}$$

If we raise both sides of the equation to (1/m)th power, we obtain

$$N \cdot (\Delta\epsilon_t)^{1/m} = C^{1/m} \tag{16}$$

or

$$N \left(\frac{\Delta\epsilon_t}{C}\right)^{1/m} = 1.0 \tag{17}$$

If we let n be the number of applications of tensile load prior to fracture, it is apparent that the lowest possible number of n is 1 while the counterpart for N generally has been taken as 1/4 or 1/2 in the literature. The difference between n and N is small at large values of N so for all practical purposes, Eq. (17) may be rewritten as follows:

$$n \left(\frac{\Delta\epsilon_t}{C}\right)^{1/m} = 1.0 \tag{18}$$

Furthermore, since at n = 1

$$\Delta\epsilon_t = \Delta\epsilon_{t1}$$

Eq. (17) becomes

$$n \left(\frac{\Delta\epsilon_t}{\Delta\epsilon_{tl}}\right)^{1/m} = 1.0 \qquad (19)$$

The slopes of the curves in Figs. 48 and 49 are approximately -1 and -1/2 respectively for test results of Evans[5] and those of Coffin[11,13]. Since Evans conducted his tests with tensile loadings only and Coffin conducted most of his tests under fully reversed-strain conditions, it seems reasonable to assume that this slope, -m, is a variable that is dependent upon the relative-strain ratio, the ratio of the cyclic compressive change in plastic true strain to the cyclic tensile change in plastic true strain. On this basis, the inverse of the slopes of the curves in Fig. 43 have been determined and found to be 1.22, 1.43, 1.65, and 1.86 respectively for r-values of -1/4, -1/2, -3/4, and -1. When these corresponding values of 1/m and r are plotted, as shown in Fig. 52, the following relationship is obtained.

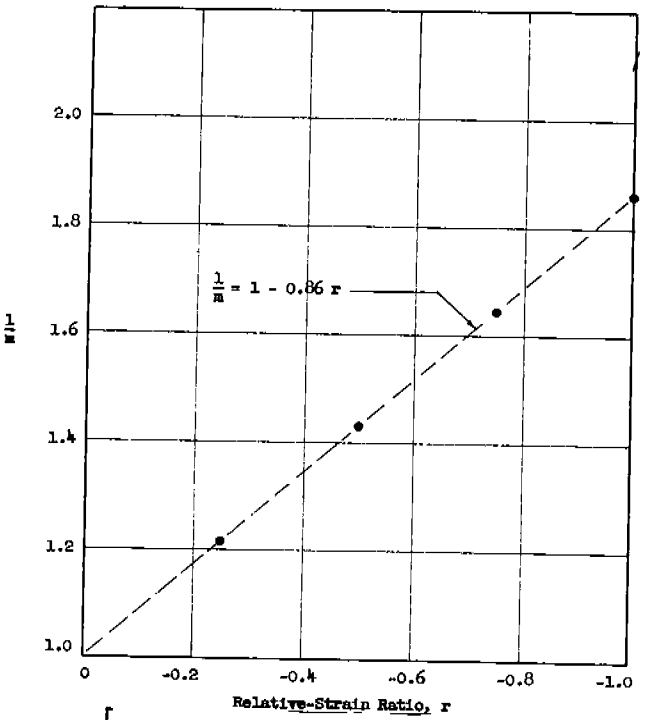

FIG. 52. VARIATIONS OF $\frac{1}{m}$ WITH RESPECT TO THE RELATIVE-STRAIN RATIO, r

$$1/m = 1 - 0.86r \qquad (20)$$

This relationship has been assumed to relate the slope of the fatigue curves to the relative-strain ratio for which they were obtained.

Several further assumptions have been made in developing a low-cycle fatigue hypothesis. Firstly, it is assumed that low-cycle fatigue fractures occur in tension only. This assumption is generally true for steels. Secondly, it is realized that the specimen geometry would change somewhat at the large plastic strains in low-cycle constant-deformation tests. However, the effect of geometrical variations in the specimen profile is assumed to be compensated when such constants as $\Delta\epsilon_{tl}$ or Δq_{tl}, as obtained from "one-cycle" test results, are used. And, finally, it is assumed that fracture of a material is produced by an accumulation of the plastic deformation experienced by the material. This assumption is made on the basis of the observations of low-cycle fatigue test data discussed earlier.

B. Hypothesis

On the basis of the experimental evidence and assumptions discussed in the previous section, it is postulated that plastic deformations cumulate according to an exponential function and more specifically, that the hypothesis may be presented in generalized form as follows:

$$\sum_{i=1}^{n} \left[\left(\frac{\Delta\epsilon_t}{\Delta\epsilon_{tl}} \right)^{1/m} \right]_i = 1.0 \qquad (21)$$

Since it has been shown[4] that for low-cycle fatigue conditions true strain values are approximately proportional to the corresponding engineering strains, a similar expression may be written as follows in terms of true strains.

$$\sum_{i=1}^{n} \left[\left(\frac{\Delta q_t}{\Delta q_{tl}} \right)^{1/m} \right]_i = 1.0 \qquad (22)$$

where $\Delta\epsilon_t$ is the cyclic tensile change in plastic engineering strain,

$\Delta\epsilon_{t1}$ is the cyclic tensile change in plastic engineering strain at n = 1,

i is the number of applications of tensile load,

n is the number of applications of tensile load prior to fracture

m is a variable depending upon the amount of cyclic compressive strain, or the relative-strain ratio,

Δq_t is the cyclic tensile change in plastic true strain,

Δq_{t1} is the cyclic tensile change in plastic true strain at n = 1.

As noted previously, both 1/m and $\Delta\epsilon_{t1}$ (or Δq_{t1}) are functions of r, the relative strain ratio. Therefore, for constant values of the relative-strain ratio, r, Eqs. (21) take the form of Eq. (19).

12. Correlations with Test Data

Six type C-2 and three type C-2A specimens of CN-steel were previously tested in reversed-load low-cycle fatigue tests. The plastic true strain history for each of these six specimens is listed in Table 8 (also see Figs. 35 and 36). By analyzing each strain-cycle with the hypothesis, the quantity

$$\sum_{i=1}^{n} \left[\left(\frac{\Delta q_t}{\Delta q_{t1}} \right)^{1/m} \right]_i$$

was evaluated for these tests and found to vary from 0.94 to 1.08 as shown in Table 8. These values are close to the value of 1.0 required by the hypothesis.

Data in the literature are generally reported for cyclic strain tests conducted by cycling a specimen between a constant cyclic maximum plastic strain (q_{max} or ϵ_{max}) and a constant cyclic minimum plastic strain (q_{min} or ϵ_{min}). In most cases, the tests were started with a tensile load to produce the upper or maximum strain limit which was followed by fully reversed strains. Some

TABLE 8. ANALYSIS OF PLASTIC STRAINS FROM REVERSED-LOAD TESTS.

[Specimen No. | Test Stress ksi, S | Cycles to Failure n | $\sum_{i=1}^{n}\left[\left(\frac{\Delta q_t}{\Delta q_{t1}}\right)^{\frac{1}{m}}\right]_i$ *]

Strain History Data i(1)	-Δqc,(2)	Δqt,(3)
[C-2-CN138 ±78 2 1.004]		
1	0	16.6
2	5.3	69.8
[C-2-CN132 ±79 4 0.993]		
1	6.8	10.7
2	3.0	8.6
3	5.6	10.1
4	7.2	73.4
[C-2-CN135 ±74 6 1.029]		
1	0	10.4
2	5.5	7.3
3	4.5	7.1
4	6.2	8.0
5	6.2	10.3
6	5.9	69.4
[C-2-CN133 ±74 16 1.022]		
1	5.8	7.3
2	3.4	5.8
3	2.9	5.9
4	4.9	4.9
5	3.9	5.8
6	3.8	5.0
7	5.0	6.5
8	5.6	6.5
9	5.5	6.4
10	5.5	6.4
11	5.4	6.3
12	5.4	6.3
13	4.5	7.1
14	4.2	7.7
15	6.8	10.1
16	6.6	65.9

Strain History Data i(1)	-Δqc,(2)	Δqt,(3)
[C-2-CN124 ±69 34 1.075]		
1	0	8.1
2	4.7	6.1
3	4.2	2.8
4	3.7	5.1
5	5.1	5.1
6	4.2	4.2
7	4.2	5.1
8	4.6	4.6
9	3.6	3.6
10	3.6	3.6
11	4.1	4.6
12	3.7	4.6
13	4.1	4.5
14	4.1	5.0
15	5.0	5.0
16	4.1	5.0
17	5.0	5.0
18	3.6	4.9
19	4.4	4.8
20	4.4	5.3
21	5.3	5.7
22	4.8	4.8
23	3.9	5.1
24	4.7	5.9
25	5.0	5.9
26	5.1	6.3
27	5.4	5.8
28	5.3	6.5
29	6.1	7.7
30	6.5	8.0
31	5.5	6.3
32	5.1	7.4
33	6.2	8.4
34	6.4	57.8
[C-2-CN117 ±70 48 1.069]		
1	4.9	5.3
2	3.0	3.9
3	3.2	3.6
4	3.2	4.0
5	3.6	4.5
6	4.1	4.1
7	4.1	4.4
8	4.0	4.0
9	3.2	7.2
10	3.6	2.4
11	2.8	3.3
12	3.3	3.7

Strain History Data i(1)	-Δqc,(2)	Δqt,(3)
C-2-CN117 (Cont'd)		
13	4.0	4.3
14	4.0	3.7
15	3.3	3.6
16	3.2	4.1
17	3.7	4.1
18	3.7	5.0
19	4.0	4.2
20	4.2	4.2
21	3.8	4.2
22	3.4	4.2
23	3.3	4.5
24	4.2	4.2
25	3.7	4.2
26	4.2	4.6
27	4.2	4.6
28	4.1	4.9
29	4.6	5.9
30	5.4	5.4
31	4.6	4.6
32	4.2	4.2
33	3.8	4.7
34	4.3	5.3
35	4.8	5.5
36	5.1	5.9
37	4.7	4.7
38	4.2	5.1
39	4.7	5.2
40	4.8	5.1
41	4.2	5.6
42	5.2	5.7
43	5.1	6.0
44	4.9	6.3
45	5.0	7.6
46	5.8	8.7
47	7.4	10.4
48	6.5	56.5
[C-2A-CN302 ±92 16 1.056]		
1	4.6	5.6
2	3.1	6.0
3	3.9	3.9
4	3.9	4.9
5	3.9	4.8
6	3.8	4.8
7	4.8	5.7
8	3.8	4.7
9	4.7	5.6
10	4.6	5.5
11	5.5	7.3
12	6.4	6.4
13	4.5	5.4
14	4.5	7.1
15	5.3	7.0
16	5.2	20.0

Strain History Data i(1)	-Δqc,(2)	Δqt,(3)
[C-2A-CN310 ±87 23 1.083]		
1	0	6.7
2	3.7	3.7
3	4.2	4.2
4	3.7	3.7
5	3.7	5.0
6	4.6	4.6
7	4.1	4.7
8	4.7	4.7
9	4.2	4.6
10	5.6	5.6
11	5.6	6.6
12	5.1	5.1
13	4.2	4.6
14	4.6	4.2
15	3.3	4.6
16	4.1	5.0
17	4.5	4.9
18	4.5	4.5
19	4.5	5.0
20	4.1	4.1
21	3.6	5.3
22	4.8	8.2
23	5.1	13.1
[C-2A-CN306 ±87 29 0.943]		
1	4.1	5.1
2	2.6	3.6
3	3.2	3.7
4	3.5	4.0
5	3.5	3.5
6	3.0	3.9
7	3.4	3.4
8	3.4	3.9
9	3.9	3.9
10	3.4	3.4
11	3.4	3.9
12	3.4	3.4
13	3.4	3.8
14	3.3	3.8
15	3.8	3.8
16	3.3	4.3
17	3.8	3.8
18	3.8	3.8
19	3.4	4.3
20	4.3	4.3
21	3.8	3.8
22	3.3	4.2
23	3.7	3.7
24	2.8	3.2
25	3.2	4.2
26	4.2	4.6
27	4.6	4.2
28	3.2	5.9
29	4.6	15.0

* See Eq. 22

(1) Number of applications of tensile load.

(2) Cyclic compressive change in plastic true strain, percent.

(3) Cyclic tensile change in plastic true strain, percent.

test series were carried out with constant absolute-strain ratios, i.e., R = constant; while others were carried out with constant mean strains, i.e., q_m or $\epsilon_m = 0$. Since the quantity Δq_t is not necessarily a constant in these tests, the test results are presented in terms of q_{max} vs. n (for positive q_{max}) or q_{min} vs. n (for negative q_{max}).

Based on the general hypothesis presented herein, equations have been derived for various test conditions. For constant R-ratios the relationship between q_{max} and n may be derived as follows: (a) The first cycle (see insert of Fig. 53) is assumed to consist of a single tensile change in plastic true strain, i.e., r = 0. (b) The subsequent cycles of strain are full-reversals, i.e., r = -1. Then, for the first cycle, (i = 1),

$$r = 0,\ 1/m = 1.0 \text{ (from Eq. 20)}$$

$$\Delta q_{t1} = q_f$$

$$\Delta q_t = q_{max}$$

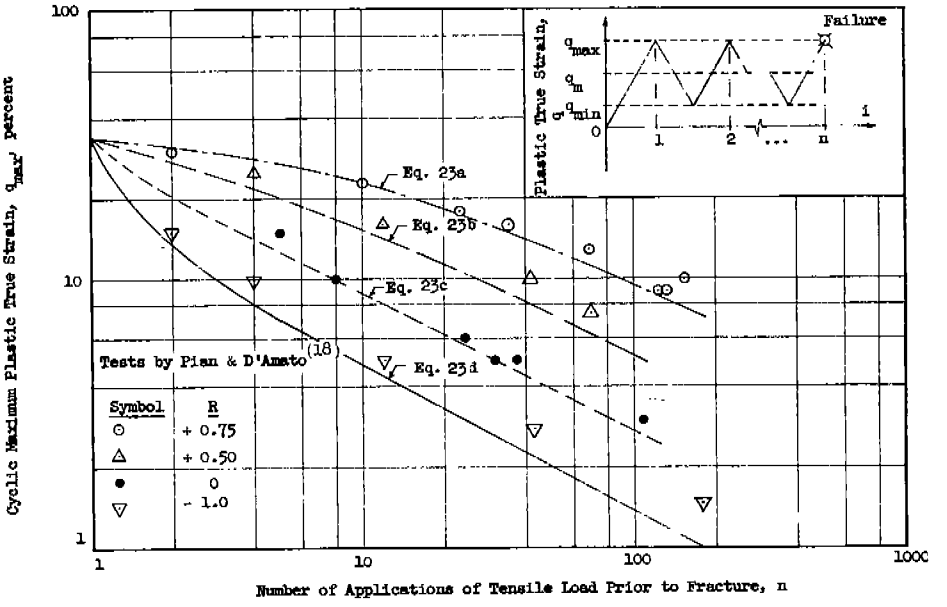

FIG. 53. CORRELATION OF HYPOTHESIS WITH VARIOUS CONSTANT - R - RATIO TESTS ON 2024 ALUMINUM ALLOY.

For the subsequent cycles ($i > 1$),

$$r = -1,\ 1/m = 1.86 \text{ (from Eq. 20)}$$

$$\Delta q_t = q_{max} - q_{min}$$

$$= (1 - R)\, q_{max}$$

If we substitute these conditions into Eq. (22), we obtain,

$$\frac{q_{max}}{q_f} + (n - 1)\left[(1 - R)\frac{q_{max}}{\Delta q_{t1}}\right]^{1.86} = 1.0 \qquad (23)$$

Pian and D'Amato[18] tested coupon-type 2024 aluminum alloy specimens with constant R-ratios of +0.75, +0.50, 0, and -1.0. The plastic true strain at simple tensile fracture, q_f, for this particular type of specimen was found to be approximately 34 percent. Since no "one-cycle" test information is available for this specimen, it is assumed that Δq_{t1} is a constant and equal to q_f for all ratios, i.e., $\Delta q_{t1} = q_f = 34$ percent. Then, from Eq. (22), the following relationships may be obtained:

For R = +0.75,
$$\frac{q_{max}}{34} + (n - 1)\left[\frac{q_{max}}{136}\right]^{1.86} = 1.0 \qquad (23a)$$

For R = +0.50,
$$\frac{q_{max}}{34} + (n - 1)\left[\frac{q_{max}}{68}\right]^{1.86} = 1.0 \qquad (23b)$$

For R = 0,
$$\frac{q_{max}}{34} + (n - 1)\left[\frac{q_{max}}{34}\right]^{1.86} = 1.0 \qquad (23c)$$

For R = -1,
$$\frac{q_{max}}{34} + (n - 1)\left[\frac{q_{max}}{17}\right]^{1.86} = 1.0 \qquad (23d)$$

These equations are plotted in Fig. 53 along with the corresponding test data taken from Ref. 18. Despite the assumption made regarding Δq_{t1}, the curves

plotted on the basis of this hypothesis seem to fit the test points reasonably well for lives up to approximately 200 cycles. Similar equations were obtained and compared with Gerberich's test data. These latter comparisons are shown in Figs. 54 and 55.

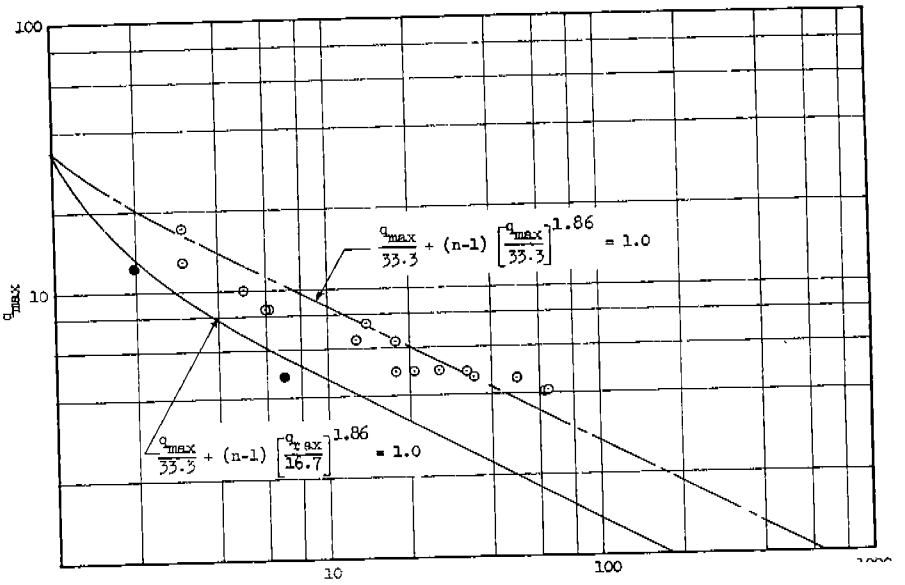

FIG. 54. CORRELATION OF HYPOTHESIS WITH VARIOUS CONSTANT -R- RATIO TESTS ON 2024 ALUMINUM ALLOY.

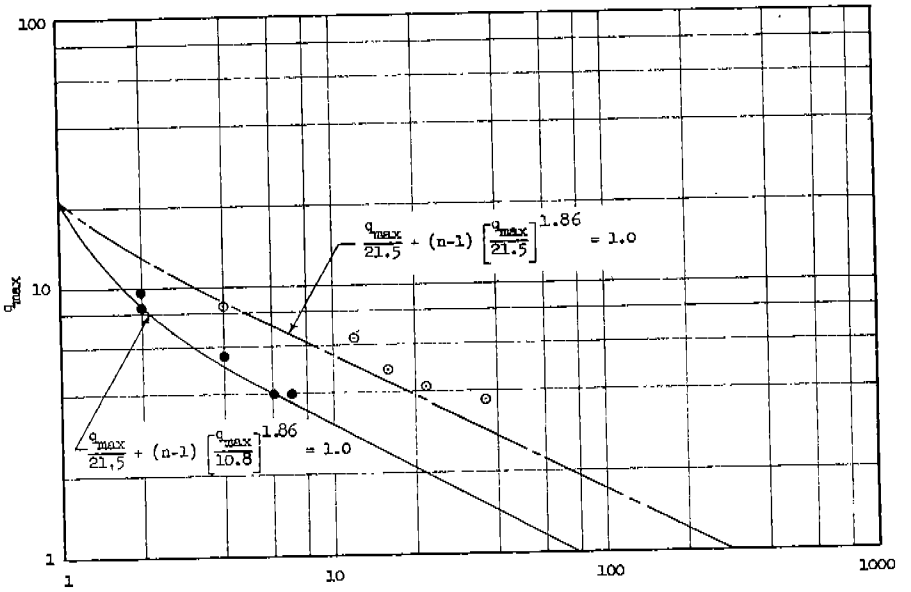

FIG. 55. CORRELATION OF HYPOTHESIS WITH VARIOUS CONSTANT -R- RATIO TESTS ON 2024 ALUMINUM ALLOY.

Similarly, expressions may be obtained for tests conducted with constant mean strains, q_m or ϵ_m.

$$q_m = \frac{1}{2}(q_{max} + q_{min}) \tag{24}$$

For the first cycle (i = 1),

$$r = 0, \qquad 1/m = 1.0 \text{ (from Eq. 20)}$$

$$\Delta q_{t1} = q_f$$

$$\Delta q_t = q_{max}$$

For the subsequent cycles (i > 1),

$$r = -1, \qquad 1/m = 1.86 \text{ (from Eq. 20)}$$

$$\Delta q_t = 2(q_{max} - q_m) = 2(q_m - q_{min})$$

Substituting these conditions into (22), we obtain

$$\frac{q_{max}}{q_f} + (n - 1)\left[\frac{2(q_{max} - q_m)}{\Delta q_{t1}}\right]^{1.86} = 1.0 \tag{25}$$

For tests with a negative mean strain and a negative maximum strain, the first load is in compression, such as shown in the insert of Fig. 56. Assuming that $\Delta q_c \cong \Delta q_t$ in the first cycle, the following equation may be obtained from Eq. (22).

$$n\left[\frac{2(q_m - q_{min})}{\Delta q_{t1}}\right]^{1.86} = 1.0 \tag{26}$$

Then, for q_m = -7.5 percent,

$$n\left[\frac{-7.5 - q_{min}}{19}\right]^{1.86} = 1.0 \tag{26a}$$

Equation (26a) is plotted in Fig. 56 in terms of q_{min} and n along with the corresponding test data from D'Amato[4]. Excellent correlations are again obtained.

D'Amato[4] reported also test results on a 2024 aluminum alloy with constant mean strains of +27.5%, +13.5%, +7.5%, 0%, and -7.5%. The plastic true strain at simple tension fracture, q_f, was found to be about 38%. Assuming again that $\Delta q_{tl} = q_f = 38\%$ for all r-values, the following equations may be obtained from Eqs. (25) and (26).

$$\text{For } q_m = +27.5\%, \qquad \frac{q_{max}}{38} + (n-1)\left[\frac{q_{max} - 27.5}{19}\right]^{1.86} = 1.0 \qquad (25a)$$

$$\text{For } q_m = +13.5\%, \qquad \frac{q_{max}}{38} + (n-1)\left[\frac{q_{max} - 13.5}{19}\right]^{1.86} = 1.0 \qquad (25b)$$

$$\text{For } q_m = +7.5\%, \qquad \frac{q_{max}}{38} + (n-1)\left[\frac{q_{max} - 7.5}{19}\right]^{1.86} = 1.0 \qquad (25c)$$

$$\text{For } q_m = 0\%, \qquad \frac{q_{max}}{38} + (n-1)\left[\frac{q_{max}}{19}\right]^{1.86} = 1.0 \qquad (25d)$$

$$\text{For } q_m = -7.5\%, \qquad n\left[\frac{-7.5 - q_{min}}{19}\right]^{1.86} = 1.0 \qquad (26a)$$

Equations (25a) through (25d) are plotted in Fig. 57 in terms of q_{max} and n, along with the corresponding test data from Ref. 4. Equation (26a) is plotted in Fig. 56 in terms of q_{min} and n along with the corresponding test data from the same reference. Excellent correlations are found in most cases.

Dubuc[16] tested SAE 1030 steel specimens with a gage length of 1 in. These tests, with $\epsilon_m = 0$, were conducted by controlling the total engineering strain range. To apply the present hypothesis, $\Delta\epsilon_{tl}$ was assumed to be constant

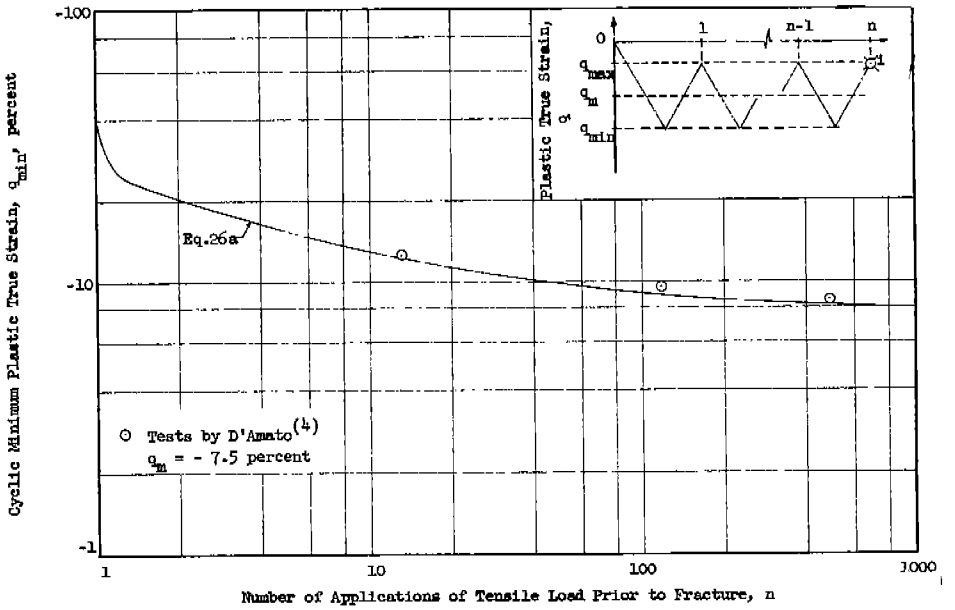

FIG. 56. CORRELATION OF HYPOTHESIS WITH NEGATIVE MEAN-STRAIN TESTS ON 2024 ALUMINUM ALLOY.

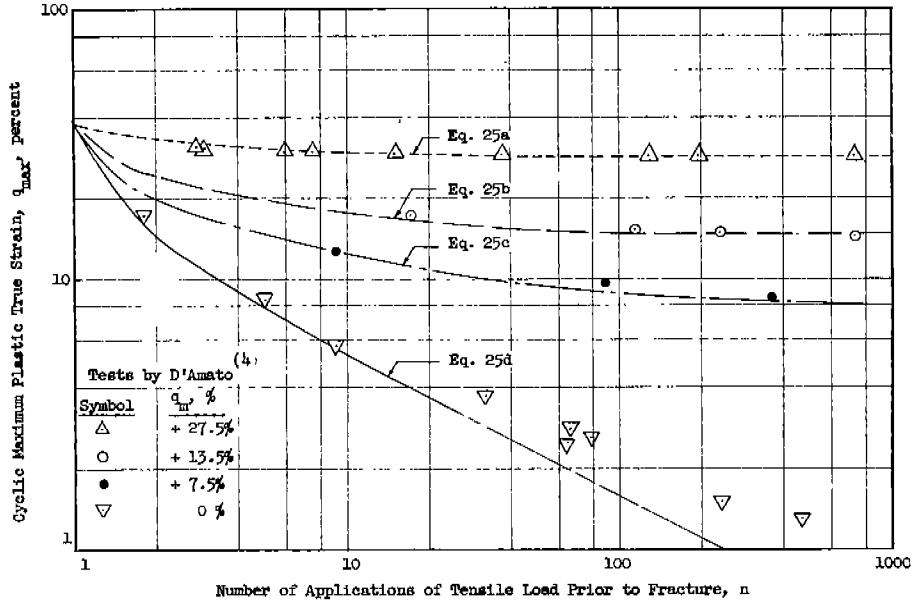

FIG. 57. CORRELATION OF HYPOTHESIS WITH VARIOUS CONSTANT-MEAN-STRAIN TESTS ON 2024 ALUINUM ALLOY.

and equal to the elongation at static tensile fracture, 44 percent in this case. Then from Eq. (25), assuming q_{max} and ϵ_{max} to be approximately equal, we obtain,

$$\frac{\epsilon_{max}}{44} + (n - 1)\left[\frac{\epsilon_{max}}{22}\right]^{1.86} = 1.0 \qquad (25e)$$

Equation (25e) is plotted in Fig. 58. In the figure, test points from Ref. 16 are plotted in terms of the cyclic maximum plastic engineering strain measured at half of the specimen life.

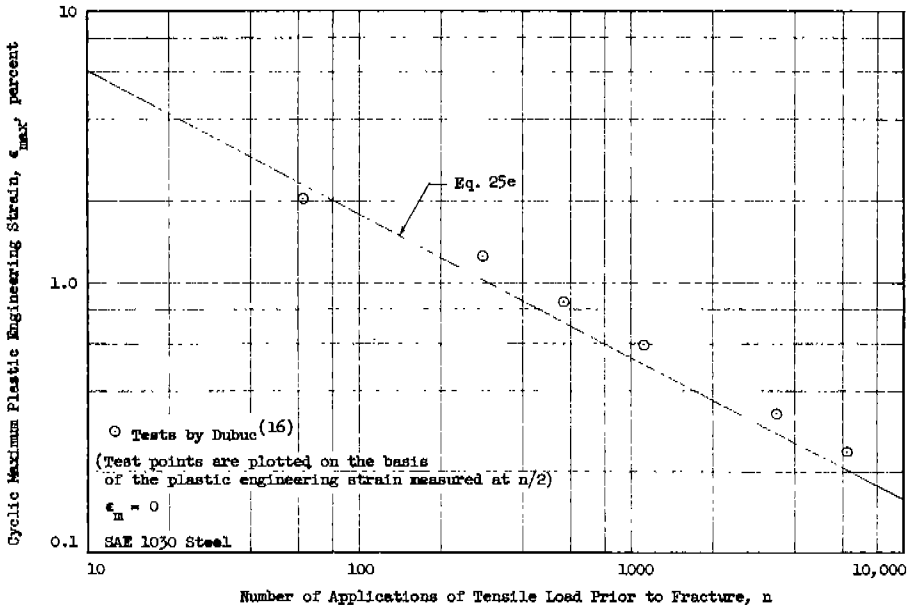

FIG. 58. CORRELATION OF HYPOTHESIS WITH TESTS CONDUCTED ON THE BASIS OF ENGINEERING STRAINS.

V. SUMMARY OF RESULTS AND CONCLUSIONS

13. General Discussions

In general, the correlations of the present hypothesis with the test results of Pian and D'Amato[18], Gerberich[27,28], and D'Amato[4] show that it may be possible to use this hypothesis to describe the cumulative low-cycle fatigue behavior of 2024 aluminum alloy specimens. In addition, the correlation

made with Dubuc's[16] test data indicates that the hypothesis may be equally applicable to tests of steel specimens conducted on the basis of engineering strains.

Since there is no available information on "one-cycle" tests of the 2024 aluminum alloy and the SAE 1030 steel, it was necessary to make the assumption that $\Delta q_{t1} = q_f$ for all r-ratios. Moreover, the use of Eq. (20), the empirical relationship obtained from the cyclic true-strain tests of mild steel specimens, may not be applicable to these materials. Nevertheless, these comparisons demonstrate that there is an excellent possibility of this hypothesis describing the general trend of low-cycle fatigue behavior of various metals under various testing conditions.

In addition to the development of the general low-cycle fatigue hypothesis, limited studies have been made on such factors as type of test, mode of failure, material, and property variations during the tests. These items will be briefly discussed in the following paragraphs.

It was considered desirable in this investigation to test all specimens under axial-loadings. Tests conducted in this manner are the simplest and provide the most direct way of obtaining the low-cycle fatigue resistance of the material. Since axial-load low-cycle fatigue tests may be carried out by controlling either the load limits or the deformation limits, both cyclic "load" and cyclic "deformation" tests were conducted. In addition, a number of one-cycle tests were carried out to establish the fatigue behavior at the lowest possible number of cycles for both the load and deformation types of tests. The latter type of test is especially worthy because it is relatively simple to perform and the results may be used in the proposed hypothesis to predict the low-cycle fatigue behavior of specimens of the same material and geometry.

In long-life fatigue tests, the fracture of a notched specimen usually exhibits little deformation. However, the fractures resulting from low-cycle fatigue loadings may show deformations which range from that of a long-life

fatigue failure to that of a static tension failure, depending upon such factors as the type of test, the magnitude of the applied stresses, the material, the geometry of the specimen, the test temperature, the cyclic rate, etc.

The effect of strain aging was considered in both one-cycle tests and reversed-load fatigue tests. In both types of tests, there was little or no difference in the low-cycle fatigue behavior of aged and unaged specimens of ABS-C normalized steel.

The three materials used in this program were all mild steels, but with different mechanical properties. While pre-compression had different effects on the one-cycle behavior of these steels, there was little or no difference in the "normalized" cyclic-deformation behavior among these three materials.

The variations in true stresses and strains that occur in both the cyclic load and the cyclic deformation tests have been studied by measuring successively the variations in strain and load after each loading. It is found that when the load-limits are maintained constant in low-cycle fatigue tests the true strain limits increase continuously until failure. In the case of cyclic deformation tests, wherein the cyclic strains are maintained constant, the true stresses in each cycle increase with the number of load applications. However, the amount of increase appears to be a function of the relative strain ratio.

14. Summary of Results

The results of this study, although based on a very limited number of tests, appear to be quite consistent and may be briefly summarized as follows:

A. One-Cycle Tests

For the two types of specimen and three steels studied in this investigation, it has been found that Δq_{t1}, the total tensile change in plastic true strain at n = 1, decreased somewhat as q_{c1}, the plastic true pre-compressive

strain was increased and also as the stress concentration of the notched specimen was increased. However, the magnitude of the decrease differed for the three steels studied. This is clearly shown in Fig. 22. It was found also that greater ultimate strengths, in terms of engineering stress, were obtained for specimens subjected to large pre-compressions as shown in Fig. 23.

B. Cyclic Load Tests

The low-cycle portion of the s-n curve resulting from zero-to-tension fatigue tests is rather flat. This suggests that the maximum engineering stress may not be a good discriminator of low-cycle fatigue life or behavior. As shown in Figs. 27 through 29, the strain at the first maximum load is a more sensitive parameter than the maximum engineering stress for the evaluation of fatigue data with lives of less than 100 cycles.

From limited test information, it is found that the time at the maximum load in each cycle has a marked effect on the low-cycle fatigue life in zero-to-tension fatigue tests.

In reversed-load tests, specimens polished in the longitudinal direction were found to be stronger in fatigue strength than those polished in the transverse direction. It was found also that the specimen with a higher stress concentration begins with a higher strength at n = 1, and then at longer lives gradually becomes less strong than the plain specimens. (See Figs. 33 and 34.)

C. Cyclic Deformation Tests

For constant relative-strain ratios, r, linear relationships of various slopes were found to exist on log Δq_t vs. log n diagrams. When these test data are analyzed on the basis of normalized cyclic tensile change in plastic strain and n, there does not seem to be any material effect on the slope of the relationships. A linear relationship was found to exist between the inverse of the slope, 1/m, and the relative-strain ratio, r.

In addition, plastic strain-histories obtained from six cyclic load tests were analyzed on the basis of the low-cycle fatigue hypothesis presented herein. With the data from these tests it was found that the condition specified by the low-cycle hypothesis was satisfied. Correlations with other published test data indicate that it may be possible also to apply the hypothesis to cyclic strain tests to metals other than mild steel.

15. Conclusions

On the basis of the information presented herein it may be concluded that, under low-cycle fatigue conditions,

(1) The tensile change in plastic true strain, Δq_{tl}, varies with the amount of plastic true pre-compressive strain, q_{cl}; the pattern of this variation is dependent on the material and the geometry of the member.

(2) A linear relationship exists between log Δq_t and log n for a constant value of relative-strain ratio.

(3) A linear relationship exists also between the quantities 1/m and r, and, for mild steel, may be expressed as follows:

$$\frac{1}{m} = 1 - 0.86r \tag{20}$$

From the above conditions a general hypothesis describing the cumulative effect of plastic deformations on the low-cycle fatigue behavior of metals has been developed and may be expressed as follows:

$$\sum_{i=1}^{n} \left[\left(\frac{\Delta q_t}{\Delta q_{tl}} \right)^{1/m} \right]_i = 1.0 \tag{22}$$

Thus, under low-cycle fatigue conditions any tensile change in plastic strain is cumulative and the manner in which this accumulation takes place is dependent upon the amount of compressive plastic strain in each cycle.

With this hypothesis a "one-cycle" test may be used to describe,

on the basis of the relative-strain ratio, the basic low-cycle fatigue behavior of mild steel for lives up to approximately 1,000 cycles. A limited number of correlations were obtained for other materials and indicate that the hypothesis may express also the low-cycle fatigue behavior of other metallic alloys. However, additional confirmations of this correlation would be desirable.

REFERENCES

1. Yao, J. T. P., and Munse, W. H., "Low-Cycle Fatigue of Metals--Literature Review," The Welding Journal, 41:4, Research Supplement, p. 182s (1962).

2. Lin, H., and Kirsch, A. A., "An Exploratory Study on High-Stress Low-Cycle Fatigue of 2024 Aluminum Alloy in Axial Loading," (WADC TN 56-317), August 1956.

3. MacGregor, C. W., "Relations Between Stress and Reduction in Area for Tensile Tests of Metals," Trans. AIME, vol. 124, p. 208, (1937).

4. D'Amato, R., "A Study of the Strain-Hardening and Cumulative Damage Behavior of 202-T4 Aluminum Alloy in the Low-Cycle Fatigue Range," (WADD TR 60-175), April 1960.

5. Evans, E. W., "Effect of Interrupted Loading on Mechanical Properties of Metals," The Engineer (London), 203:5274, Part I, p. 293; 203:5275, Part II, p. 325 (1957).

6. Kommers, T. B., "Repeated Stress Testing," New York: International Association for Testing Materials (VIth Congress), 1912.

7. Low, A. C., "The Bending Fatigue Strength of Aluminum Alloy MG5 Between 10 and 10 Million Cycles," Jour. Roy. Aeronautic Soc., vol. 59, p. 502 (1955).

8. Low, A. C., "Short Endurance Fatigue," International Conference on Fatigue of Metals, p. 206, 1956.

9. Johansson, A., "Fatigue of Steels at Constant Strain Amplitude and Elevated Temperatures," Stockholm: Colloquium on Fatigue (IUTAM), 1956.

10. Coffin, L. F., Jr., and Read, J. H., "A Study of the Strain Cycling and Fatigue Behavior of a Cold-Worked Metal," International Conference on Fatigue, p. 415, 1957.

11. Coffin, L. F., Jr., and Tavernelli, J. F., "The Cyclic Straining and Fatigue of Metals," Trans. Metallurgical Society of AIME, vol. 215, p. 794 (October 1959).

12. Coffin, L. F., Jr., "The Stability of Metals under Cyclic Plastic Strain," Journal of Basic Engineering, 82:3, ser. D, p. 671 (September 1960).

13. Tavernelli, J. F., and Coffin, L. F., Jr., "A Compilation and Interpretation of Cyclic Strain Fatigue Tests on Metals," Trans. ASM, vol. 51, p. 438 (1959).

14. Douglas, D. A., and Swindeman, R. W., "The Failure of Structure Metals Subjected to Strain Cycling Conditions," (Paper 58-A-198), ASME, 1958.

15. Majors, H., Jr., "Thermal and Mechanical Fatigue of Nickel and Titanium," Trans. ASM, vol. 51, p. 421 (1959).

16. Dubuc, J., Plastic Fatigue under Cyclic Stress and Cyclic Strain with a Study of the Bauschinger Effect (Ph.D. Thesis submitted to Ecole Polytechnique, Universite de Montreal, Montreal, Canada), January 1961.

17. Liu, S. I., Lynch, J. J., Ripling, E. J., and Sachs, G., "Low-Cycle Fatigue of the Aluminum Alloy 24S-T in Direct Stress," Metals Technology, February 1948.

18. Pian, T. H. H., and D'Amato, R., "Low-Cycle Fatigue of Notched and Unnotched Specimens of 2024 Aluminum Alloy under Axial Loading (WADC TN 58-27), 1958.

19. Sachs, G., Gerberich, W. W., and Weiss, V., Low-Cycle Fatigue of Pressure Vessel Materials, Interim Technical Report No. 5 (Report No. MET575-601IT5, Metallurgical Research Laboratories). Syracuse: Syracuse University Research Institute, January 1960.

20. Sachs, G., Gerberich, W. W., Weiss, V., and Latorre, J. V., "Low-Cycle Fatigue of Pressure-Vessel Materials," Proc. ASTM, vol. 60, p. 512 (1960).

21. Mehringer, F. J., and Felgar, R. P., "Low-Cycle Fatigue of Two Nickel-Base Alloys by Thermal-Stress Cycling," Journal of Basic Engineering, 82:3, ser. D, p. 661 (September 1960).

22. Orowan, E., "Theory of the Fatigue of Metals," Proc. Roy. Soc., A171, p. 79, 1939.

23. Orowan, E., "Stress Concentrations in Steel under Cyclic Loading," The Welding Journal, 31:6, Research Supplement, p. 273, 1952.

24. Gross, J. H., Stout, R. D., "Plastic Fatigue Properties of High-Strength Pressure Vessel Steels," The Welding Journal, 34:4, Research Supplement, p. 161s (1955).

25. Manson, S. S., Behavior of Materials under Conditions of Thermal Stress (NACA TN 2933), 1953.

26. Martin, D. E., "An Energy Criterion for Low-Cycle Fatigue," Journal of Basic Engineering, Trans. ASME, April 1961.

27. Gerberich, W. W., The Phenomena of Cumulative Damage in Stress Cycling and Strain Cycling Fatigue, Interim Technical Report No. 3 (Report No. MET575-594T3, Metallurgical Engineering Dept.), Syracuse: Syracuse University Research Institute, April 1959.

28. Gerberich, W. W., An Analysis of Several of the Variables Encountered in Low-Cycle Fatigue, Interim Technical Report No. 4 (Report No. MET575-5961T4, Metallurgical Engineering Dept.), Syracuse: Syracuse University Research Institute, June 1959.

29. Bridgman, P. W., "Studies in Large Plastic Flow and Fracture," McGraw-Hill Book Co., 1952.

30. Drucker, D. C., Mylonas, C., and Lianis, G., "On the Exhaustion of Ductility of E-Steel in Tension Following Compressive Pre-Strain," The Welding Journal, 39:3, Research Supplement, p. 117s (March 1960).

31. Zener, C., "The Micro-Mechanism of Fracture," Fracturing of Metals, ASM, 1948.

APPENDIX

Notations

A_c Cross-sectional area at the test section of the specimen after pre-compression, sq. in.

A_f Cross-sectional area at the test section of the specimen at fracture, sq. in.

A_o Original cross-sectional area at the test section of the specimen, sq. in.

A_r Cross-sectional area at the test section of the specimen, re-machined after pre-compression, sq. in.

C A constant

d_c Diameter at the test section of the specimen after pre-compression, in.

d_f Diameter at the test section of the specimen at fracture, in.

d_o Original diameter at the test section of the specimen, in.

d_r Diameter at the test section of the specimen, in., re-machined after pre-compression

i Number of applications of tensile load

n Number of applications of tensile load prior to fracture

N Number of cycles

N_c Number of cycles to crack initiation

N_f Number of cycles to fracture

q Plastic true strain, percent

q_{cl}	Plastic true pre-compressive strain, percent
q_f	Plastic true strain at fracture in simple tension, percent
q_m	Mean cyclic plastic true strain, percent
q_{max}	Cyclic maximum plastic true strain, percent
q_{min}	Cyclic minimum plastic true strain, percent
q_{tl}	Plastic tensile true strain at fracture, percent
r_q	Relative-strain ratio; cyclic compressive change in plastic true strain to cyclic tensile change in plastic true strain, $\Delta q_c/\Delta q_t$
R_q	Absolute-strain ratio, cyclic minimum plastic true strain to cyclic maximum plastic true strain, q_{min}/q_{max}
R_s	Stress ratio, cyclic minimum engineering stress to cyclic maximum engineering stress, s_{min}/s_{max}
s	Engineering stress, ksi
s_c	Engineering stress at the maximum compressive load, ksi
s_{max}	Maximum engineering stress, ksi
s_{min}	Maximum engineering stress, ksi
s_u	Ultimate strength, ksi
Δq_c	Cyclic compressive change in plastic true strain, percent
Δq_t	Cyclic tensile change in plastic true strain, percent
Δq_{tl}	Total tensile change in plastic true strain at n=1, percent
$\Delta \epsilon_c$	Cyclic compressive change in plastic engineering strain, percent
$\Delta \epsilon_t$	Cyclic tensile change in plastic engineering strain, percent
$\Delta \epsilon_{tl}$	Total tensile change in plastic engineering strain at n=1, percent
ϵ_f	Plastic engineering strain at fracture, percent
ϵ_m	Mean plastic engineering strain, percent
σ	True stress, ksi
σ_c	True stress at the maximum compressive load, ksi
σ_f	True stress at fracture, ksi

☆ U.S. GOVERNMENT PRINTING OFFICE : 1963 O - 691-734

NATIONAL ACADEMY OF SCIENCES-NATIONAL RESEARCH COUNCIL

Committee on Ship Structural Design